Grant Agreement Number: 952183
Project Acronym: BOW
Project Full Title: Biogenic Organotropic Wetsuits
Start date of the project: November 1st, 2020
Duration: 48 months
Project Coordinator: Paolo Bergese (CSGI)
Project Officer: Ioannis Amarantos
Project Website: www.bowproject.eu
Project e-mail address: bow@csgi.unifi.it

D1.7: Functionalization of EVs

DELIVERABLE INFORMATION	
Deliverable N°	1.7
Deliverable Title	Functionalization of EVs
WP N°	1
Lead beneficiary	MPG
Contributing partners	CNR, CSGI, RR
Type	Report
Lead authors	Ana Mateos Maroto (MPG), Svenja Morsbach (MPG)
Due Submission Date	30/04/2023
Actual Submission Date	28/04/2023

TYPE		
R	Document, report	☒
DEM	Demonstrator, pilot, prototype	☐
DEC	Websites, patent filing, videos, etc.	☐
OTHER		☐

DISSEMINATION LEVEL

This project has received funding from the European Union's Horizon 2020 research and innovation programme under grant agreement No 952183

PU	Public	☒
PP	Restricted to other programme participants (incl. Commission Services)	
RE	Restricted to a group specified by the consortium (incl. Commission Services)	
CO	Confidential, only for the members of the consortium (incl. Commission Services)	

STATUS	
Draft	
Final	☒

REVISION HISTORY		
Date	**Authors and Contributors**	**Comments**
22/03/2023	Ana Mateos Maroto (MPG), Svenja Morsbach (MPG)	Draft
19/04/2023	Andrea Zendrini (CSGI), Paolo Bergese (CSGI)	First revised version
27/04/2023	Ana Mateos Maroto (MPG), Svenja Morsbach (MPG), Katharina Landfester (MPG)	Second draft
28/04/2023	Ana Mateos Maroto (MPG), Svenja Morsbach (MPG), Andrea Zendrini (CSGI), Paolo Bergese (CSGI), Antonalla Bongiovanni (CNR), Giorgia Adamo (CNR)	Final version

GLOSSARY OF TERMS	
Term	**Definition**
AB	Antibody
ApoA1	Apolipoprotein A1
$CHCl_3$	Chloroform
Chol	Cholesterol
cryoTEM	Cryogenic Transmission Electron Microscopy
DBCO	Dibenzylcyclooctyne
D_h	Hydrodynamic Diameter
DiR	1,1'-Dioctadecyl-3,3,3',3'-tetramethylindotricarbocyanine iodide
DLS	Dynamic Light Scattering
DMSO	Dimethyl Sulfoxide

This project has received funding from the European Union's Horizon 2020 research and innovation programme under grant agreement No 952183

DOPE	1,2-Dioleoyl-*sn*-glycero-3-phosphoethanolamine
MSC	Endometrial Tissue derived Mesenchymal Stem Cell
RBCs	Red Blood Cell
eggPC	L-α-phosphatidylcholine (Egg, Chicken)
evMBDs	Extracellular Vesicle membrane coated Magnetic Bead Devices
EVs	Extracellular Vesicles
Fc	Crystallizable Fragment (Antibody)
HPLC	High Performance Liquid Chromatography
MALDI-TOF	Matrix-Assisted Laser Desorption/Ionization Time-of-Flight mass spectrometry
MFI	Mean Fluorescence Intensity
MWCO	Molecular Weight Cut-Off
NA	Nanoalgosomes
PBS	Phosphate Buffered Saline w/o Ca, Mg
PdI	Polydispersity Index
PEG	Poly(ethylene glycol)
RBC	Red Blood Cells
RT	Room Temperature
sec AB	Secondary Antibody
SR-B1	Scavenger Receptor Class B type 1
SPAAC	Strain-promoted Alkyne-Azide Click

This project has received funding from the European Union's Horizon 2020 research and innovation programme under grant agreement No 952183

The statements made herein do not necessarily have the consent or agreement of the BOW consortium.

This project has received funding from the European Union's Horizon 2020 research and innovation programme under grant agreement No 952183

INDEX

This project has received funding from the European Union's Horizon 2020 research and innovation programme under grant agreement No 952183

1. INTRODUCTION

BOW aims at exploring and consolidating the technology able to recapitulate key natural biomimetic functions – including camouflage to the immune system and organ site/tumor-targeting – to synthetic nanomaterials and nanodevices by transferring on them membranes of extracellular vesicles (EVs). Part of the research activity has been devoted to exogenous functionalization of the membrane of the featured EVs to further augment their natural targeting ability. This deliverable, D1.7, reports about the results obtained during the first 24 months of activity on this specific objective. Activity has been developed within WP 1 (Separation, engineering and grading of EVs from human mesenchymal stromal/stem cells (MSCs) and microalgae), *Task 1.3: EV membrane engineering for augmented targeting*.

The devised strategy for EV functionalization has been divided in two parts, aiming at two different types of targeting agent to be bound to the membranes: 1) functionalization with proteins and 2) functionalization with small molecules. This has been done to provide a versatile functionalization platform able to cover a range of final applications.

To employ previously developed experience, focusing on specific applications within the expertise of the Consortium, we have decided to focus on the following targeting structures (sketched in Fig. 1):

- Apolipoprotein A1 (ApoA1) – a "don't eat me"- signalling protein, isolated from human plasma, potentially enabling targeting of SR-B1 receptors in brain tissue/transport across the blood brain barrier (BBB) and also inducing the so-called "stealth" effect (reduced unspecific cellular uptake and thus longer blood circulation times).
- Folate – a small molecule binding to folate receptor β presented on profibrotic macrophages.

This project has received funding from the European Union's Horizon 2020 research and innovation programme under grant agreement No 952183

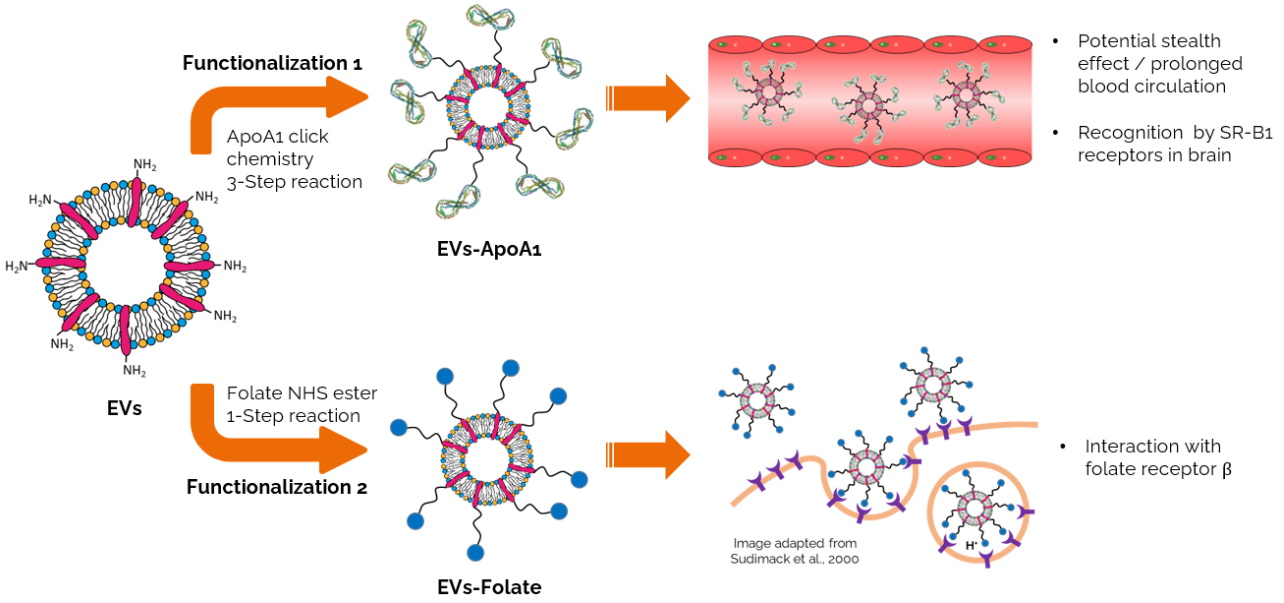

Figure 1. Overview of the functionalization strategies and structures.

Functionalization with ApoA1 has been successfully applied to EVs from Endometrial Tissue derived Mesenchymal Stem Cells (MSCs) and from red blood cells (RBCs) (Sections 4.1.1 and 4.1.2). Functionalization with folate has been successfully applied on model liposomes (Sections 4.2.1) and tested on nanoalgosomes (Section 4.2.2), but it will be soon extended also to EVs derived from MSCs and from RBCs.

Note that the use of RBC derived EVs (provided by CSGI partner) was not expected in the work plan described in the grant agreement (GA). They have been introduced as a contingency plan to cope with the fact that for about 5 months (October 2022 – March 2023) the Consortium had to face severe shortage of MSC derived EVs, due to the change of the partner in charge of their production (from RIGENERAND/EVOTEC to University of Modena and Reggio Emilia). In view of the encouraging results, as those presented in the following, and of their translational potential – also recognized by the external scientific advisory board: "In the perspective of the member of the advisory board, the pursued "fall back strategies" such as RBC derived EVs could hold major potential for clinical application" – RBC derived EVs have been now added in the pipeline of the project activities.

Finally, it has to be mentioned that, especially regarding folate functionalization, several months, about 6, of delay due to the COVID19 pandemic had to be dealt with. In particular, mainly the procurement of chemicals and lab consumables was affected, and we faced long shipping times for deliveries from outside of the EU.

This project has received funding from the European Union's Horizon 2020 research and innovation programme under grant agreement No 952183

2. RATIONALE

The coupling of ApoA1 to EVs from microalgae (nanoalgosomes) was investigated and developed on nanoalgosomes in the framework of the VES4US project on a small scale. Thus, the aim of the part 1 of functionalization task was to transfer the functionalization procedure to the other EV types and optimize it for larger scale production.

The part 2 of the functionalization task is on the development on the EV functionalization with folate and subsequent testing *in vitro* and *in vivo*, which will be performed by HGMU partners within WP4, where the corresponding model systems for lung fibrosis are available. The desired route for nanodevice administration in this case is inhalation in contrast to intravenous injection as planned for ApoA1-functionalized EVs.

For both functionalization routes, initial testing was and is performed on liposomal model systems, which allow for production of large sample amounts that are ideal for method optimization. In this deliverable we present the optimization of EV functionalization with ApoA1 as well as the strategy validation for folate coupling on model liposomes and further the transfer to nanoalgosomes.

For the successful functionalization of EVs, a thorough characterization of available functional groups is required. For both proposed functionalization strategies, we rely on the surface-bound amino groups of membrane proteins or lipids. Therefore, before performing any kind of membrane modification, in a first step the number of amino groups in each sample needs to be precisely quantified. This is done via a fluorescamine assay, which is already outlined in D1.5 "Minimal analytical package for assessment of EVs" and will be later described in detail (section 4.1.1). Subsequently, depending on the strategy, the chemical modifications of the membranes are performed as outlined below.

2.1 EV FUNCTIONALIZATION WITH PROTEINS

For the functionalization with proteins, we rely on a conjugation strategy using the strain-promoted alkyne-azide click (SPAAC) chemistry approach. The procedure mainly consists of three steps (Fig. 2): 1) azidation of the protein (in this case ApoA1), 2) modification of the EV membrane with DBCO groups (strained alkyne groups) and 3) the click chemistry reaction between the azidated protein and DBCO-coupled EVs.

The key points in this approach are the physiological reaction conditions for each step, which enable to keep protein structures intact and retain biological functionality. Additionally, precise quantification of available functional DBCO groups is necessary to adjust the reaction stoichiometries and later allow for ideal purification conditions as no large excesses are required in the reactions.

This project has received funding from the European Union's Horizon 2020 research and innovation programme under grant agreement No 952183

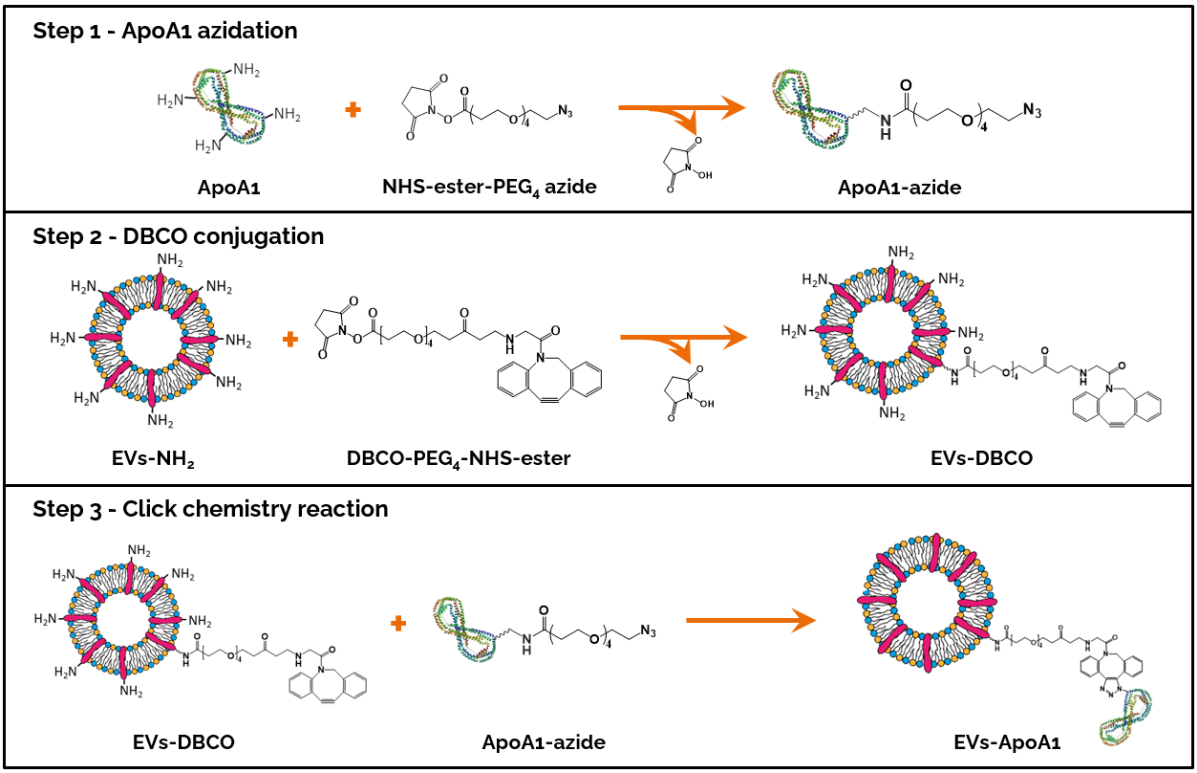

Figure 2. Functionalization strategy for conjugation of proteins to EVs *via* click chemistry.

2.2 EV FUNCTIONALIZATION WITH FOLATE

The strategy for EV functionalization with folate groups involves a one-step reaction between the EV membrane available amino groups and a folate-conjugated PEG-NHS linker (Figure 3). NHS chemistry can be performed under physiological conditions, which is also ideal for the modification of EVs. As folate is a small molecule and might be covered by proteins as soon as the carriers enter a biological milieu (formation of a protein corona), we decided to include a poly(ethylene glycol) (PEG) spacer (M_W ca. 2000 g/mol). This way, we ensure anti-fouling effect, also allowing for enough room between the target structure and the EV surface.

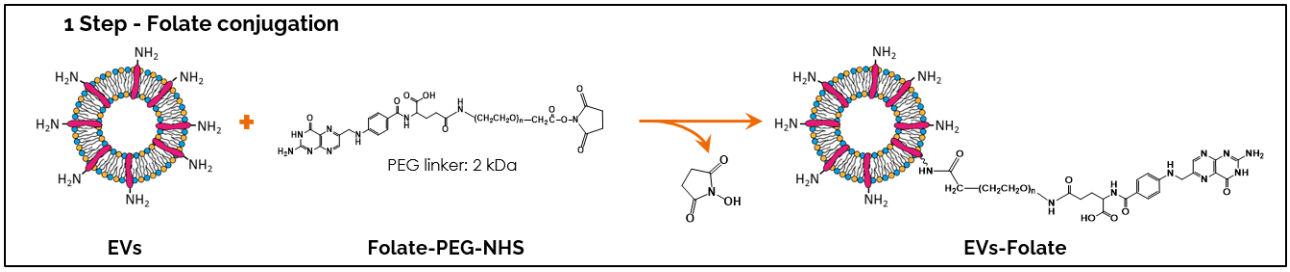

Figure 3. Functionalization strategy for conjugation with folate *via* NHS chemistry.

This project has received funding from the European Union's Horizon 2020 research and innovation programme under grant agreement No 952183

3. MATERIALS AND METHODS

3.1 EV SAMPLES

For all the functionalization strategies, experiments, testing and optimization were conducted with different EV batches. Characteristics of the specific batches used for the results reported in this deliverable are shown in Table 1.

Additional characterization data can be found in Appendix I.

Table 1. EV batches characteristics.

	Nanoalgosomes	Human EVs from mesenchymal stem cells	Human EVs from red blood cells
Sample ID	SG3	EV-3D16_1	RBC-EVs
Species of origin	*Tetraselmis chuii* culture medium	Human EDT-MSC	Red blood cells
Protein concentration	270 µg/mL	0.91 µg/µL	0.91 µg/µL
Particle concentration	6×10^{12} particles/mL	9.1×10^{11} particles/mL	3×10^{12} particles/mL
D_h (nm)	50 - 150	150 - 600	150 - 400
PdI	0.21	0.21	0.21
Zeta Potential (mV)	-24 ± 20	-17 ± 11	-26 ± 6

4. RESULTS

4.1 EV FUNCTIONALIZATION WITH PROTEINS

4.1.1 APOLIPOPROTEIN A1-FUNCTIONALIZATION OF MSC-EVs

The main functionalization strategy and proof of concept for EV functionalization with ApoA1 were developed within the frame of the VES4US project. In this project, we have now further optimized and developed the procedure to transfer the strategy to other sensitive EV sources – in this case EVs derived from mesenchymal stem cells from endometrial decidual tissue (EDT-MSCs). For each EV source, it is extremely important to verify the ideal EV functionalization parameters as the EV membranes might differ in their composition and, thus, also their stability. This later determines for example which purification protocols can be used or whether certain amounts of non-aqueous solvents can be tolerated.

As mentioned above, in a first step for every applied functionalization step, a careful analysis of available amino groups on the EV membrane surface was conducted. The procedure was already described in D1.5 and is outlined below in Fig. 4. In short, the quantification of amino groups relies on the reaction of primary amines with fluorescamine to form a fluorescent product. The resulting

This project has received funding from the European Union's Horizon 2020 research and innovation programme under grant agreement No 952183

fluorescence can be recorded at 470 nm and compared to a standard curve obtained from a serial dilution of glycine. In all assays, special attention has to be paid to other compounds in the EV samples. For instance, in the case of EDT-MSC EVs, phenol red is routinely added to the cell culture medium as a pH indicator, which is of extreme importance since at physiological pH phenol red presents absorbance peaks at 430 and 557 nm. For this reason, it is necessary to consider that remaining traces of phenol red in the medium may cause interference in the fluorescamine assay, as well as in the subsequent anthracene azide assay, which will be described later. These interferences may lead to misleading results of the assays, which can compromise the desired stoichiometry of the reactions involved in the functionalization protocol of the EVs.

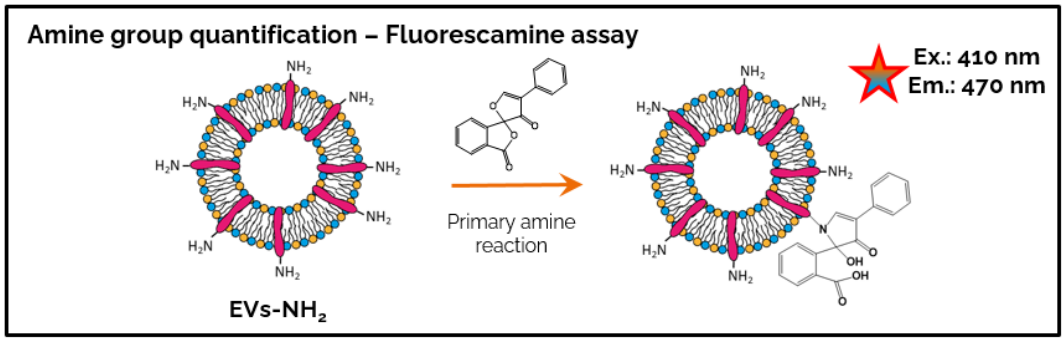

Figure 4. Procedure of MSC-EV functionalization step 1: Amine group quantification via fluorescamine assay.

In the next step, the available amino groups are reacted with a DBCO-PEG_4-NHS linker via NHS chemistry (see Fig. 5). In this way, the amino groups are transformed into strained alkyne groups, which are then available for click chemistry. For this reaction, a DBCO:NH_2 molar ratio of 5:1 was chosen. It is necessary to point out that the DBCO linker is not soluble in water, thus stock solutions were prepared in DMSO. For this reason, it is of extreme importance to optimize the amount of organic solvent to a minimum (only few microliters) to avoid possible aggregation events. The mixture was stirred at 500 rpm, at RT for 24 h. Afterwards, DBCO-EVs were purify from excess of DBCO-PEG_4-NHS by centrifugation with Amicon filters (100 kDa molecular cut-off) 3x (500 g, 30 min, RT) by PBS.

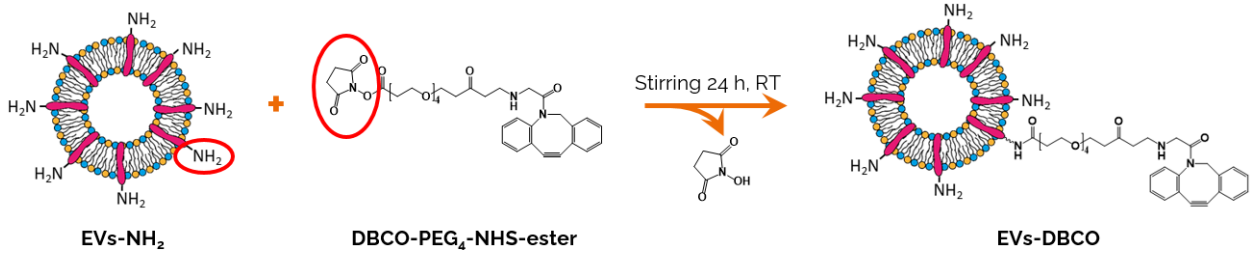

Figure 5. Procedure of MSC-EV functionalization step 2: Conjugation of DBCO-PEG-NHS linker to EV surface NH_2 groups via NHS chemistry.

After the reaction, again a quantification step is performed to analyze the number of introduced DBCO groups. This is conducted via an anthracene azide assay as shown below (Figure 6). Also here,

This project has received funding from the European Union's Horizon 2020 research and innovation programme under grant agreement No 952183

phenol red was found to be problematic. As mentioned above, the remaining traces of phenol red might interfere in the recorded emission fluorescence spectra of the anthracene azide, which may lead to inaccurate values of the number of DBCO molecules.

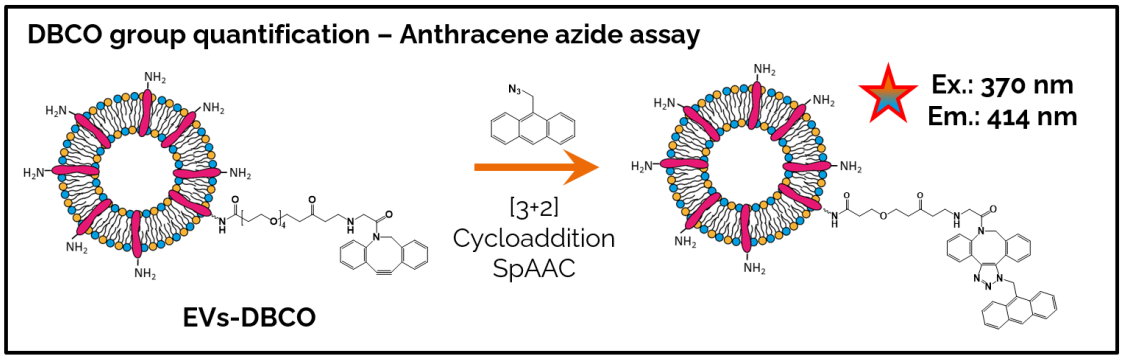

Figure 6. Procedure of MSC-EV functionalization step 3: DBCO group quantification *via* anthracene azide assay.

The results of surface group quantification of MSC-EVs before and after reaction with the DBCO linker are shown below in Figure 7. The number of detected amino groups was 1.01 x 10^6 per EV (based on a particle number of 9.1 x 10^{11} particles/mL) and the corresponding number of detected DBCO groups was 1.30 x 10^5 per EV. Generally, the number of detected DBCO groups is about one order of magnitude lower than the number of amino groups per EV. This is based on the fact that for the graphical representation we assume a constant EV particle number, which in reality is most likely not the case after the washing step. Thus, the value applied for further functionalization is the number of DBCO groups per mL and we only give groups per EV for the graphical comparison.

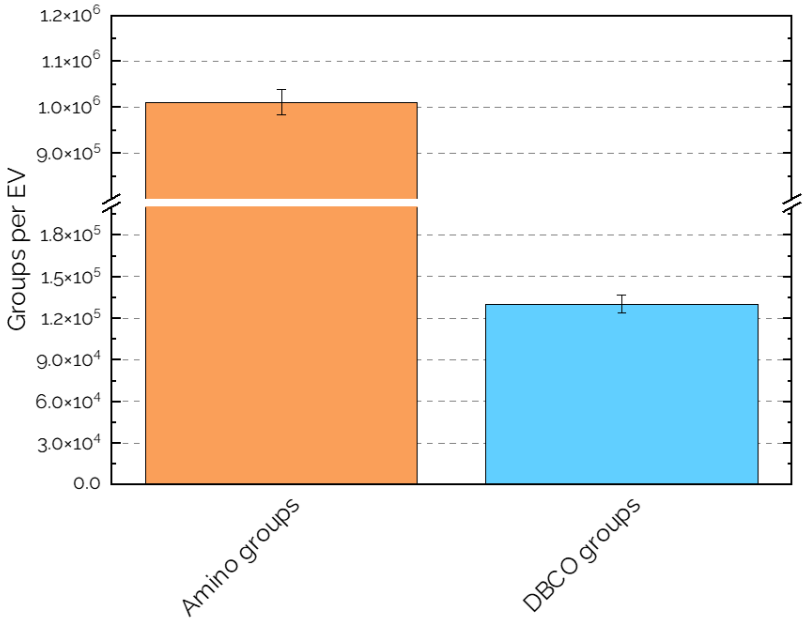

Figure 7. Quantification results of NH_2 and DBCO groups before and after MSC-EVs reaction with DBCO-PEG-NHS linker.

This project has received funding from the European Union's Horizon 2020 research and innovation programme under grant agreement No 952183

Finally, in the last step, the click reaction between azidated ApoA1 and the DBCO-conjugated EVs was performed (Fig. 8). The azidation of ApoA1 also relies on the functionalization of ApoA1 amine groups with an NHS-PEG-azide, which was already developed and optimized in the previous FET-OPEN VES4US project (D4.3. "Functionalization of microalgal EVs"). The number of introduced azide groups can be precisely tuned between 1-22 groups per protein but should be kept as low as possible to retain the natural conformation of ApoA1. In this case, a reaction stoichiometry ratio of 2:1 (ApoA1:DBCO) was chosen to allow for maximum ApoA1 functionalization. Afterwards, the excess of ApoA1 was removed by washing with Amicon filters (100 kDa molecular cut-off) 3x (500 g, 30 min, RT) by PBS. The corresponding physico-chemical characterization data (size determined by DLS and zeta potential) are shown in Table 2. We noticed that the MSC-EVs seem to be less tolerable regarding small amounts of DMSO as linker solvent, as their size distribution becomes broader and shifts a bit towards bigger sizes. This means that for this source it is extremely important to optimize the linker amount and solvent amount even further.

Figure 8. Procedure of MSC-EV functionalization step 3: Conjugation of azidated ApoA1 to DBCO-EVs via click chemistry.

Table 2. Physico-chemical characterization of MSC-EVs before and after the different functionalization steps.

Sample	Size: d (nm)	PdI	Zeta Potential (mV)
MSCS-EVS	150-600	0.21	-17 ± 11
MSC-EVs-DBCO:NH_2 **5:1**	200 - >1000	0.94	-13 ± 44
MSC-EVs-ApoA1:DBCO **2:1**	200 - >1000	0.90	-29 ± 10

Lastly, the attachment of ApoA1 was verified via flow cytometry (Figure 9), which has been proven to be a powerful tool for EV characterization[1, 2]. Additionally, it was shown to be a valuable tool for the recognition of functional groups/proteins on nanomaterials[3] and is as such routinely applied in the group at MPG[4]. In this step, a fluorescently labeled secondary antibody directed against ApoA1 is added, which binds to the ApoA1 conjugated on the EV surface. The flow cytometry protocol was previously optimized for nanoalgosomes in the VES4US project (D4.3 "Functionalization of microalgal EVs"), however it needs to be readjusted according to the specific conditions of the EV source and particle concentration. Thus, samples were incubated with and without secondary antibody for 30

This project has received funding from the European Union's Horizon 2020 research and innovation programme under grant agreement No 952183

min at 4 °C in the dark. Additionally, as controls also the unmodified and DBCO-conjugated EVs were analyzed with and without added secondary antibody. The relevant scatter plots used for the corresponding gating strategy are shown in Appendix II. As shown in Fig. 9, significant presence of secondary antibody was only found in the sample with coupled ApoA1 together with the secondary antibody. Thus, we can conclude that the modification of MSC-EVs with ApoA1 was successful.

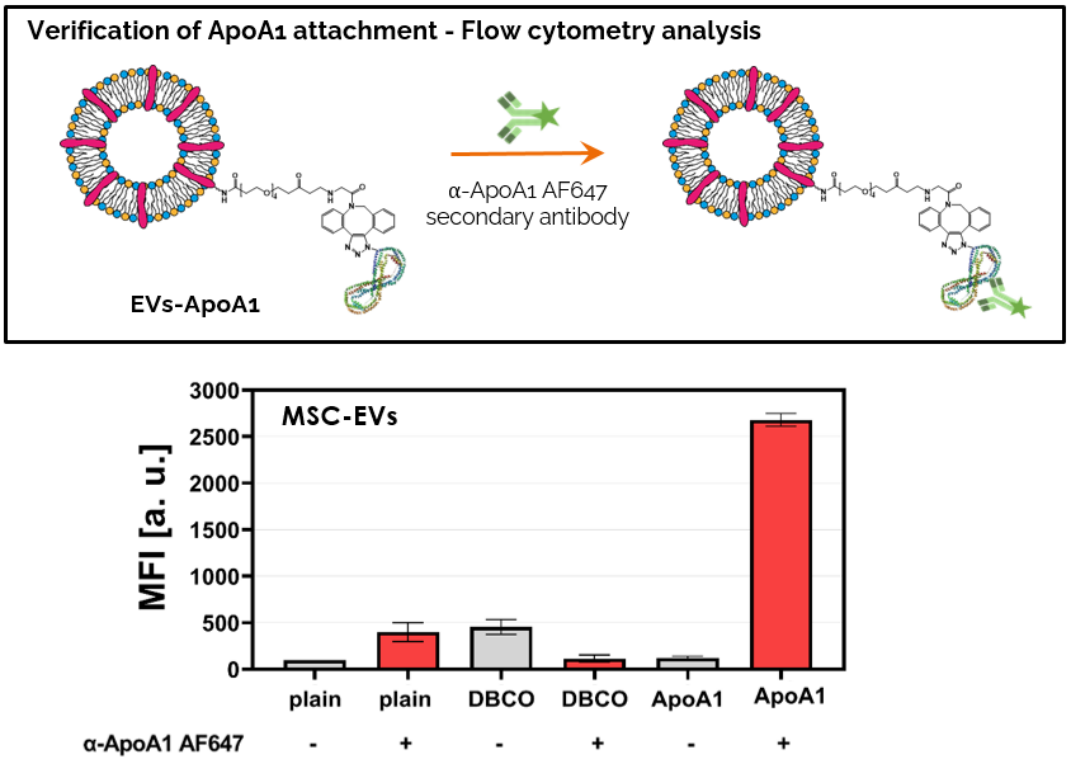

Figure 9. Verification of ApoA1 attachment to EV surfaces by flow cytometry. Samples were incubated with α-ApoA1 AF647 secondary antibodies and the corresponding results showing the mean fluorescence intensity (MFI) of each sample incubated with (+) or without (-) antibody are shown in the lower graph.

4.1.2 APOLIPOPROTEIN A1-FUNCTIONALIZATION OF RBC-EVs

Next, we have applied the same functionalization strategy to another EV source to 1) expand the library of accessible EV types even more and 2) to scale up the functionalization procedure itself. EVs from red blood cells (RBCs) are available in relatively large quantities, so that the obtained concentration is around one order of magnitude higher compared to nanoalgosomes and MSC-EVs. Therefore, although not mentioned in the original proposal, we have included this source in the functionalization plan.

In general, the same scheme described in section 4.1.1 was applied. However, as mentioned above, we wanted to further optimize the general amount of DMSO needed to dissolve the DBCO-PEG-NHS linker and, together with that the linker, amount itself. Here, we found that the reaction can be performed with a lower linker amount compared to number of amino groups (DBCO:NH_2 = 0.75:1) without any loss of function. This means that number of introduced DBCO groups saturates at this

This project has received funding from the European Union's Horizon 2020 research and innovation programme under grant agreement No 952183

ratio and higher stoichiometries or even excess is not needed. On a similar note, the reaction time could be shortened to 2 h. Below, the results obtained from the quantification of amino groups and DBCO groups is shown (see Figure 10) as well as the physico-chemical characterization data obtained from the different steps (Table 3).

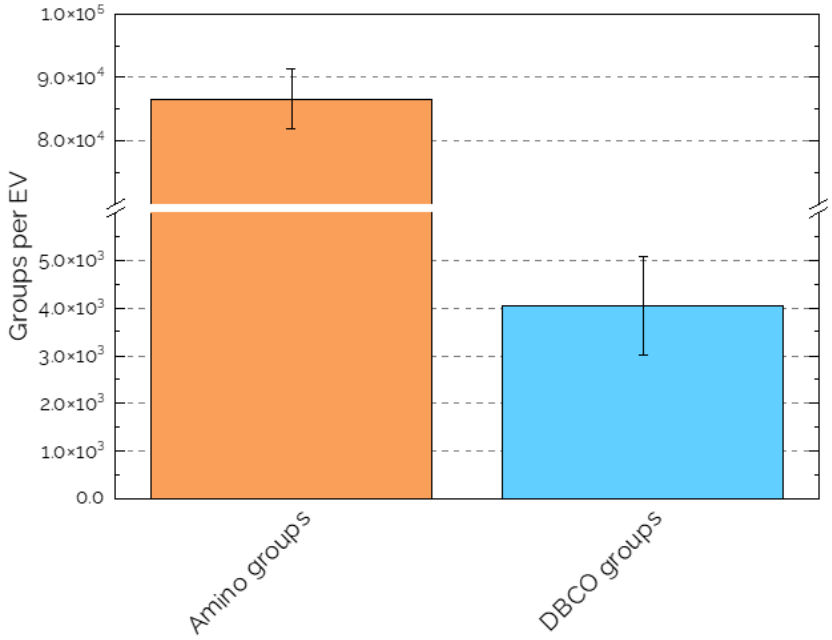

Figure 10. Quantification results of NH_2 and DBCO groups before and after RBC EV reaction with DBCO-PEG-NHS linker.

Table 3. Physico-chemical characterization of MSC-EVs before and after the different functionalization steps.

Sample	Size: d (nm)	PdI	Zeta Potential (mV)
RBC-EVs	150 - 400	0.21	-26 ± 6
RBC-EVs-DBCO:NH_2 0.75:1	150 - 400	0.18	-29 ± 4
RBC-EVs-ApoA1:DBCO 2:1	150 - >1000	0.54	-20 ± 10

From the physico-chemical characterization data, it could be seen that indeed the aggregation tendency of EVs after introduction of DBCO groups was lower as compared to MSC EVs. Thus, the chosen reaction conditions for optimization seem to be ideal, although no comparison with higher linker amounts for the same EV type is available. Afterwards, again the functionalization with ApoA1 was confirmed via flow cytometry. The results are shown in Figure 11 and the relevant scatter plots used for the corresponding gating strategy can be seen in Appendix II.

This project has received funding from the European Union's Horizon 2020 research and innovation programme under grant agreement No 952183

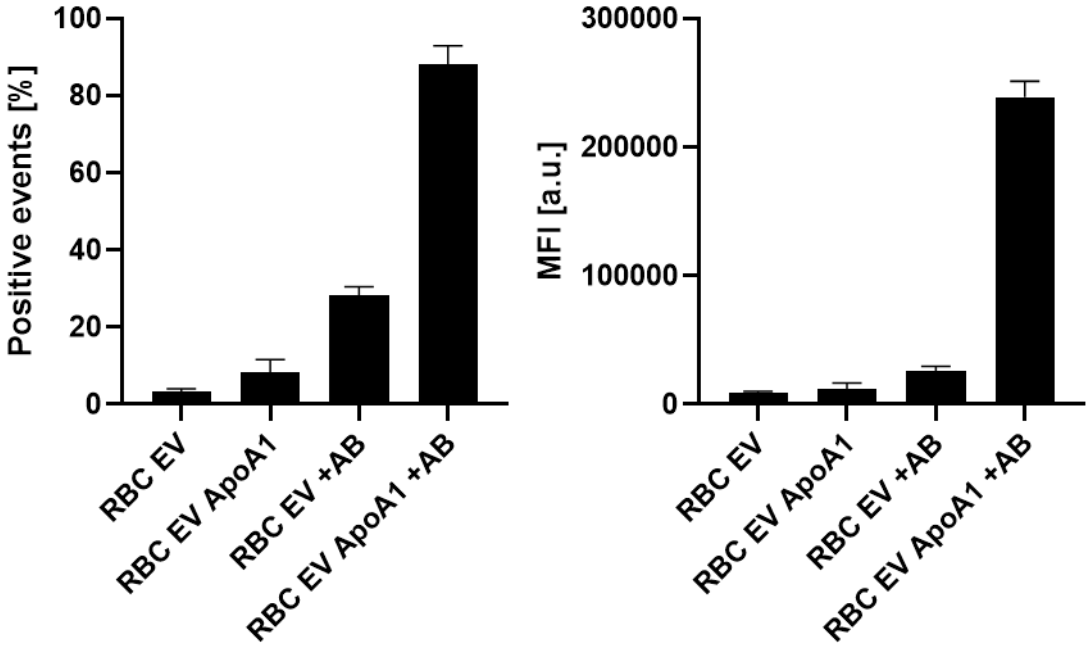

Figure 11. Verification of ApoA1 attachment to EV surfaces by flow cytometry. Samples were incubated with α-ApoA1 AF647 secondary antibodies and the corresponding results show the fraction of fluorescence positive events (left) and mean fluorescence intensity (MFI) of each sample (right) incubated with (+AB) or without antibody.

In this experiment, the highest signal (meaning highest attachment of anti-ApoA1 antibody) was obtained from the ApoA1-functionalized sample incubated with the anti-ApoA1 antibody. Therefore, we were able to verify that also in this case, we have successfully attached ApoA1 to the membrane of RBC-EVs.

4.2 EV FUNCTIONALIZATION WITH FOLATE

4.2.1 LIPOSOME MODEL SYSTEM

For the development of a new functionalization strategy, as mentioned above, we decided to use a liposomal model system, which is ideal in terms of available sample amount and physico-chemical properties. Size and membrane charge can be tuned to match the characteristics of EVs and membrane-bound amino groups can be introduced via the use of specific lipids. For our system, we chose a composition of eggPC:DOPE:cholesterol = 1:1:1, which was already found to be ideal for functionalization[4]. These lipids are mixed in organic solvent ($CHCl_3$), dried to produce a thin film and subsequently hydrated with PBS buffer (see Figure 12). After subsequent extrusion, small unilamellar liposomes are obtained.

This project has received funding from the European Union's Horizon 2020 research and innovation programme under grant agreement No 952183

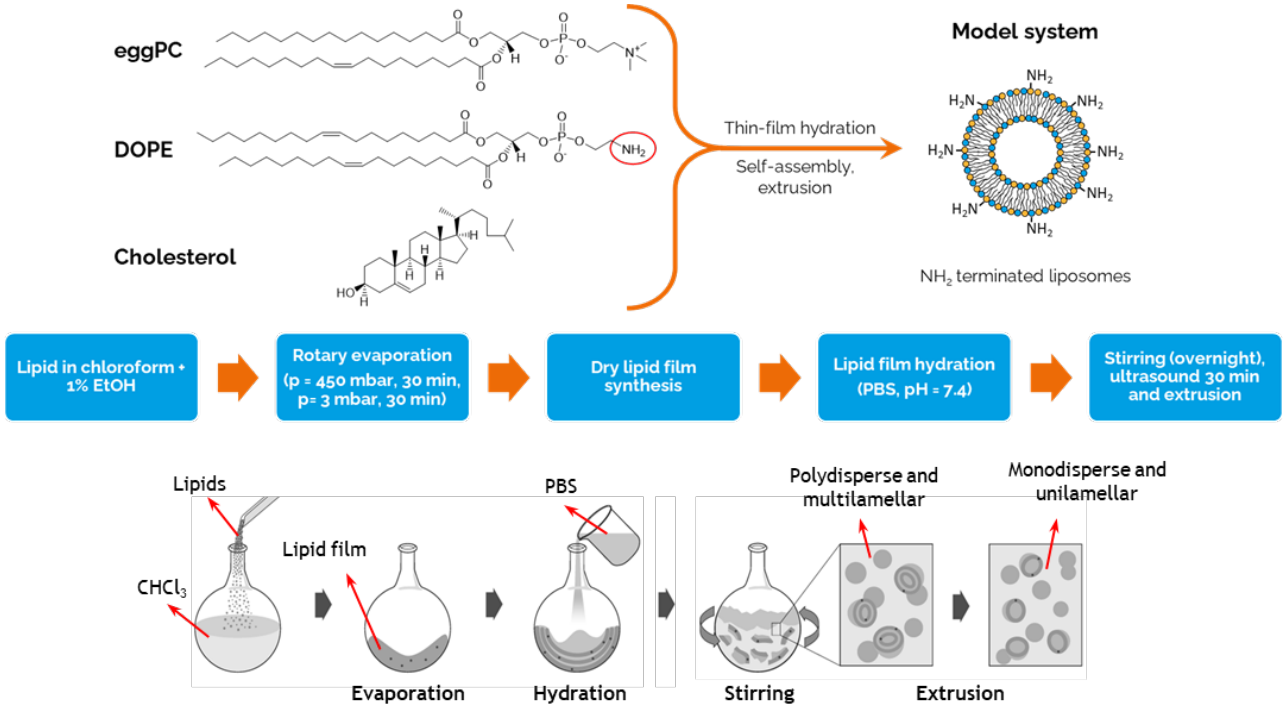

Figure 12. Composition and synthesis of model liposomes.

4.2.1.1 NHS CHEMISTRY CONJUGATION APPROACH

In our first approach, we aimed at applying a one-step functionalization approach to reduce the number of involved purification steps to a minimum. Thus, NHS chemistry was chosen (Figure 13), which is the same reaction as used for the conjugation of DBCO groups to the amine groups on lipid membrane surfaces. In this case, a commercially available folate-conjugated PEG-NHS linker with PEG chain length of 2000 g/mol was chosen. After the reaction, in principle only the *N*-hydroxy succinimide, which accumulates as a byproduct, has to be removed. In Table 4, characterization data of the liposome batch produced for the coupling reaction data reported below are shown.

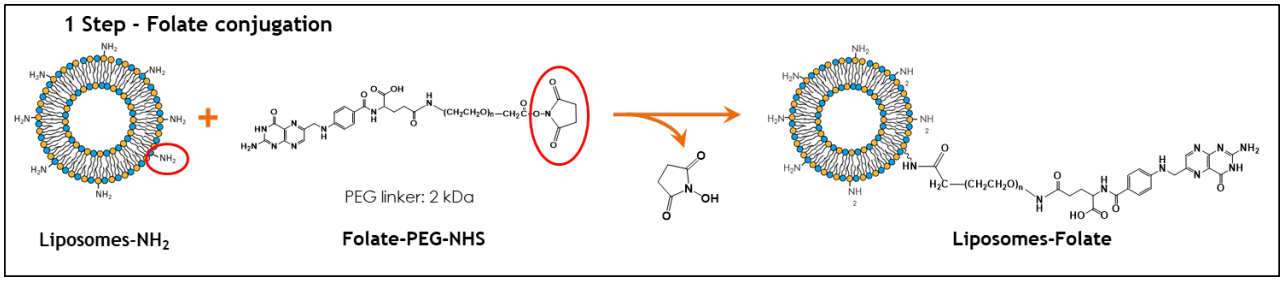

Figure 13. Functionalization reaction for folate coupling of liposomes via NHS chemistry.

This project has received funding from the European Union's Horizon 2020 research and innovation programme under grant agreement No 952183

Table 4. Physico-chemical characterization of liposomes applied for NHS coupling of folate.

Model liposomes	
Sample	eggPC:DOPE:Chol 1:1:1
Solid content	2.38 mg/mL
Particle concentration	9.65 x 10^{12} particles/mL
D_h (nm)	140 ± 2
PdI	0.1
Zeta Potential (mV)	-23 ± 7
NH_2 groups per liposome	1.28 x 10^5

To optimize the reaction and test different stoichiometric conditions, different folate:amino group ratios were chosen for the reaction, ranging from 0.5:1 to 10:1. After the reaction and corresponding washing steps (centrifugation with Vivaspin filters 300 kDa 3x at 7000 g, 4 °C for 30 min) size and charge of the obtained products were determined and are shown in Figure 14. The obtained surface charge changed towards less negative membranes, although the results showed a large standard deviation, which indicates that measurement/sample quality was not ideal. For the size measurements, slightly large sizes were obtained with higher folate ratios, but the change was not significant.

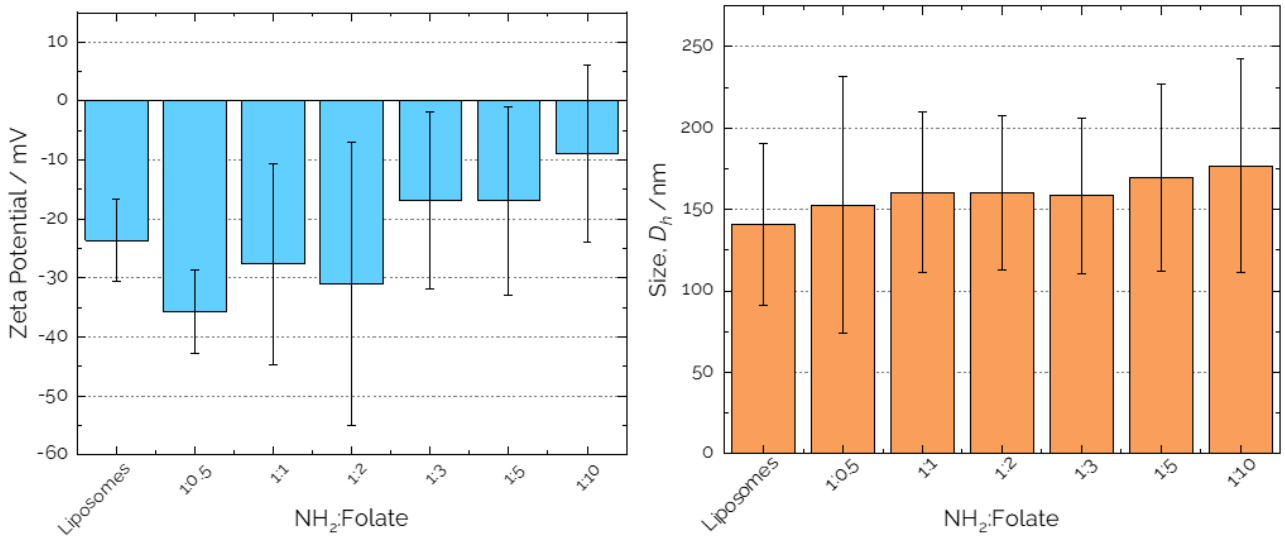

Figure 14. Physico-chemical characterization of liposomes after NHS folate coupling reaction. Left: Zeta potential, right: hydrodynamic diameter from dynamic light scattering.

This project has received funding from the European Union's Horizon 2020 research and innovation programme under grant agreement No 952183

In the next step, a method to quantify the number of introduced folate groups was established (Figure 15). For that purpose, we established a protocol based on Modupe et al[5], setting up a calibration curve based on the absorption of folic acid at a wavelength of 292 nm. The results obtained for the quantification of folate groups after the conjugation reaction are shown in Figure 16.

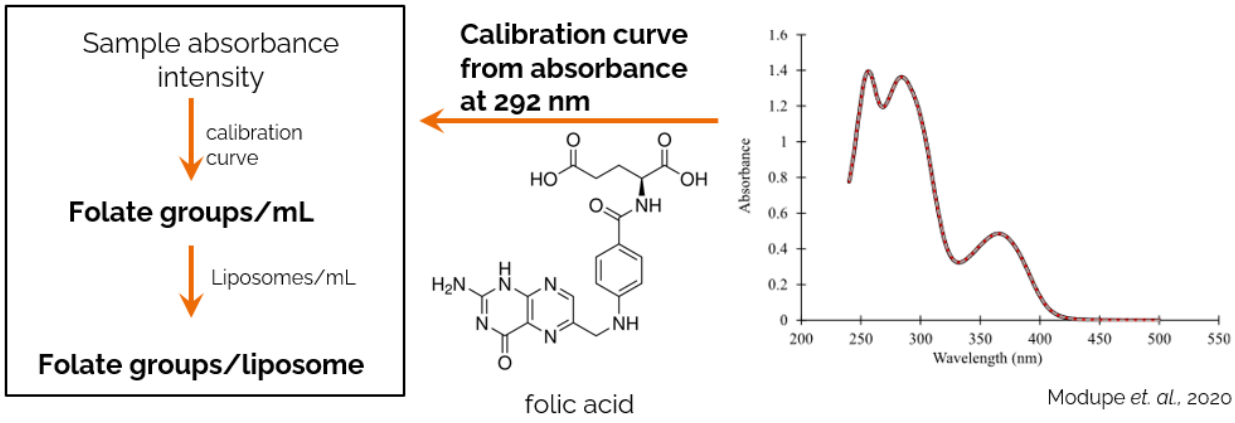

Figure 15. Quantification of folate groups – schematic procedure for absorbance measurement.

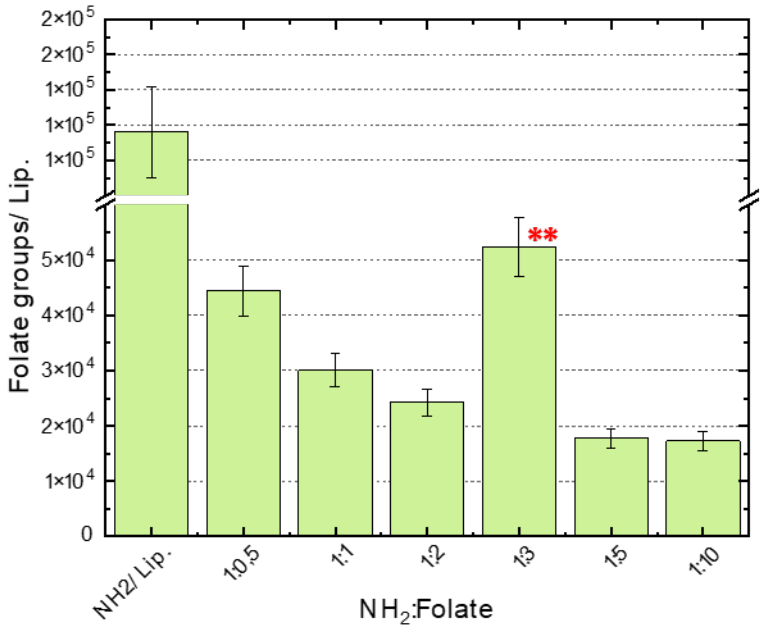

Figure 16. Quantification of folate groups results after reaction with liposomes in different stoichiometries. (** indicates sample with error in washing procedure).

Surprisingly, the number of folate groups per liposome detected in each sample decreased with higher amount of folate used in the reaction. This was rather counter intuitive and suggested that there might have been aggregate formation of the linker itself as well as increased removal during the purification. We were able to verify aggregate formation of the linker itself (without

This project has received funding from the European Union's Horizon 2020 research and innovation programme under grant agreement No 952183

addition to the liposomes) via DLS and cryo-TEM. Therefore, we subsequently tested whether any covalent binding of the folate linker to the liposomes had taken place. For that purpose, an HPLC method was developed and pure liposomes, pure folate linker as well as liposome-coupled folate linker were compared (Figure 17).

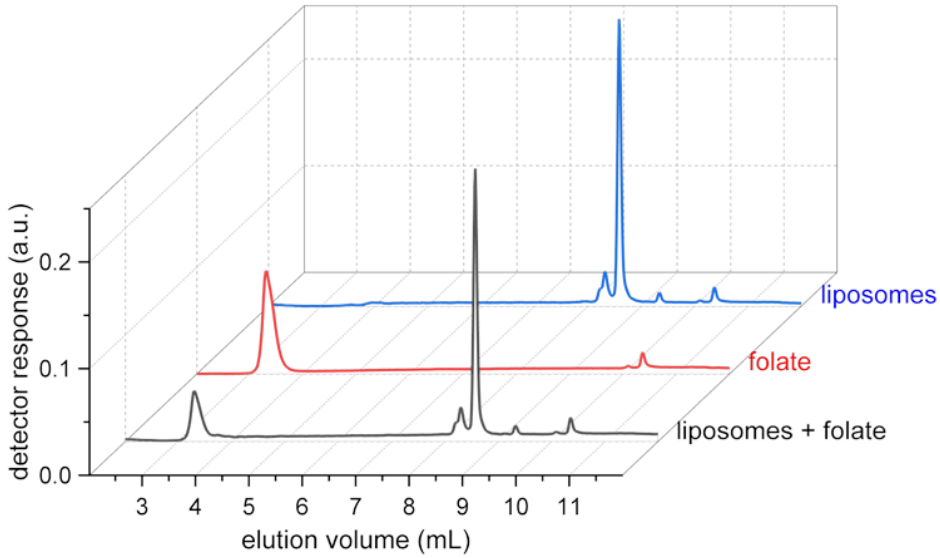

Figure 17. HPLC elugrams of unfunctionalized liposomes, pure folate linker and liposomes functionalized with folate linker via NHS chemistry.

As suspected, no covalently bound folate linker could be detected, as this should have resulted in a peak between 5-8 mL elution volume. Instead, the liposome + folate sample seems to be mixture of the pure components. After further HPLC testing, we assumed oligomerization of the folate linker due to the presence of an amino group at the folate "head" of the molecule. This group can in principle also react via NHS chemistry to that inter- or intramolecular reactions can happen. This was verified via mass spectrometry (Figure 18), where molecular masses of not only the linker itself but also 2-5x of that mass were detected in significant amounts.

This project has received funding from the European Union's Horizon 2020 research and innovation programme under grant agreement No 952183

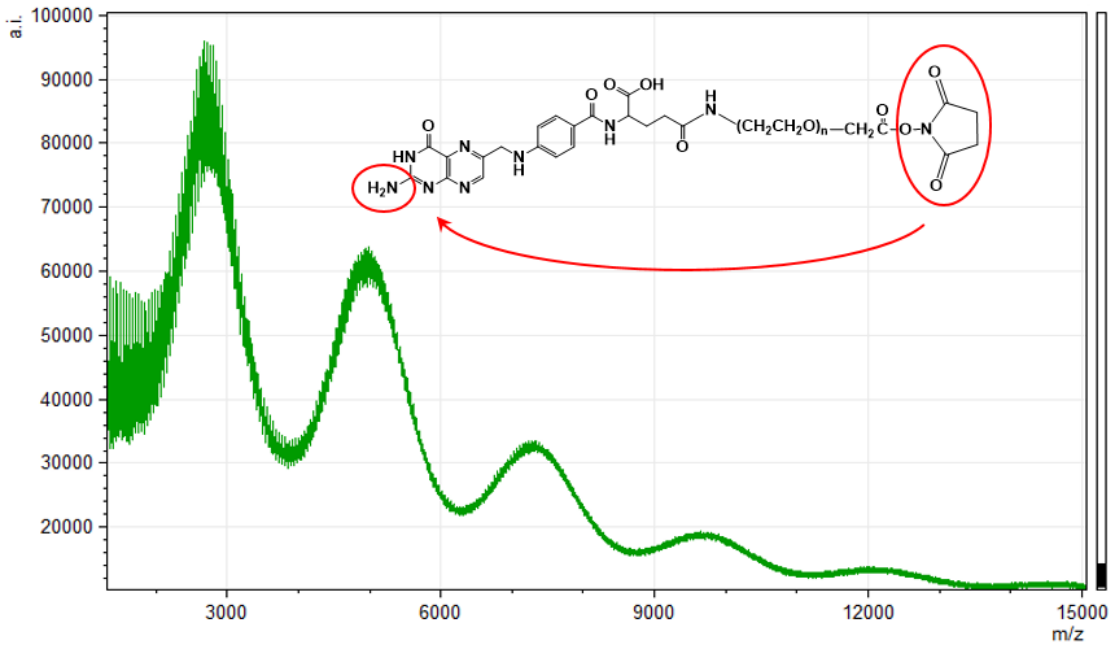

Figure 18. Mass spectrometry analysis (MALDI-TOF) of folate-PEG-NHS linker together with chemical structure and proposed oligomerization mechanism.

Further testing of the same reaction was performed with a different available linker (slightly longer PEG chain), where less oligomerization was observed. However, under reaction conditions with liposomes, still no covalent binding was observed. Also, functionalization of the pure DOPE lipid was not successful. Thus, at this point we concluded to change the functionalization strategy and also in the case of folate coupling use the well-established click chemistry approach.

4.2.1.2 CLICK CHEMISTRY

Based on the experience we have with the click chemistry approach regarding the functionalization of EVs, we now chose this approach also for the attachment of folate groups, even if this means that one more reaction and purification step needs to be included. Given the bio-orthogonal nature of the reaction, the presence of an additional amino group at the folate moiety is not a problem. Thus, the same reaction principle as outlined above was followed (see Figure 19). Instead of a folate-PEG-NHS linker, a folate PEG-azide was used. The physico-chemical properties of liposomes used for this functionalization approach are shown in Table 5.

This project has received funding from the European Union's Horizon 2020 research and innovation programme under grant agreement No 952183

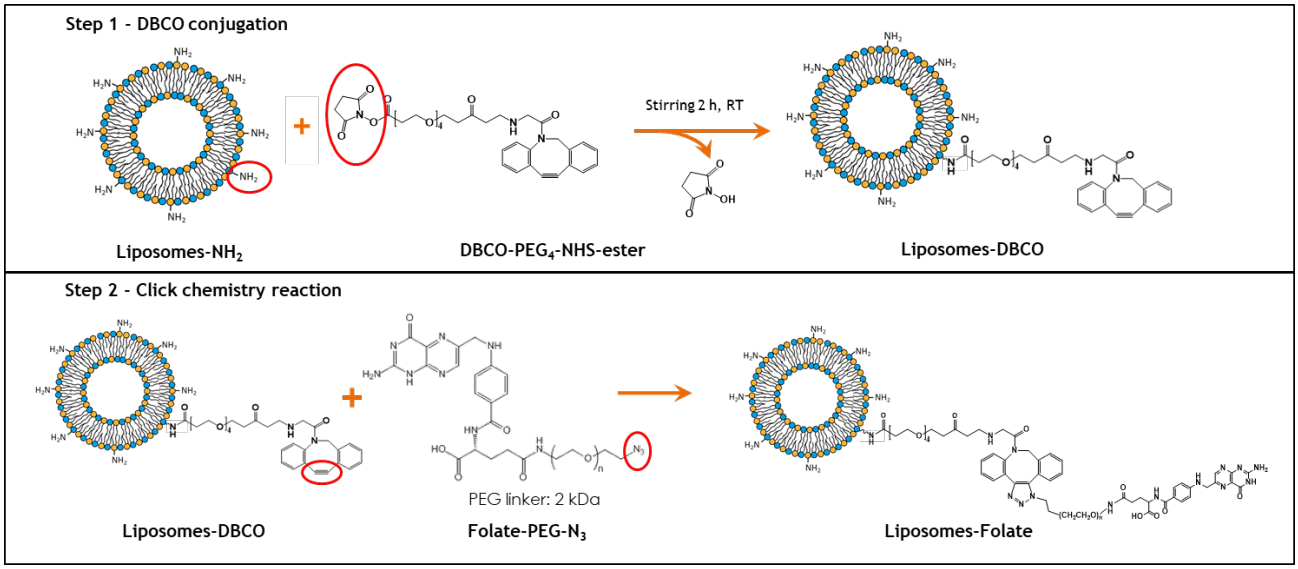

Figure 19. Functionalization reaction for folate coupling of liposomes via click chemistry.

Table 5. Physico-chemical characterization of liposomes applied for click chemistry coupling of folate.

Model liposomes	
Sample	eggPC:DOPE:Chol 1:1:1
Dye	0.1% DiR
D_h (nm)	154 ± 1
PdI	0.101
Zeta Potential (mV)	-17 ± 9
Solid content	5.9 mg/mL
Particle number	2 x 10^{13} lip./mL

As described before, quantification of amine groups and quantification of DBCO groups after the first reaction step were conducted. Results are shown in Figure 20 below. Then, the conjugation with the folate-PEG-azide linker was again performed with different DBCO groups:folate reaction ratios (1:0.5 – 1:10). As before, all samples were characterized regarding size and surface charge after the reaction and purification (Figure 21). Slight changes in zeta potential and size were visible, but they were not significant.

This project has received funding from the European Union's Horizon 2020 research and innovation programme under grant agreement No 952183

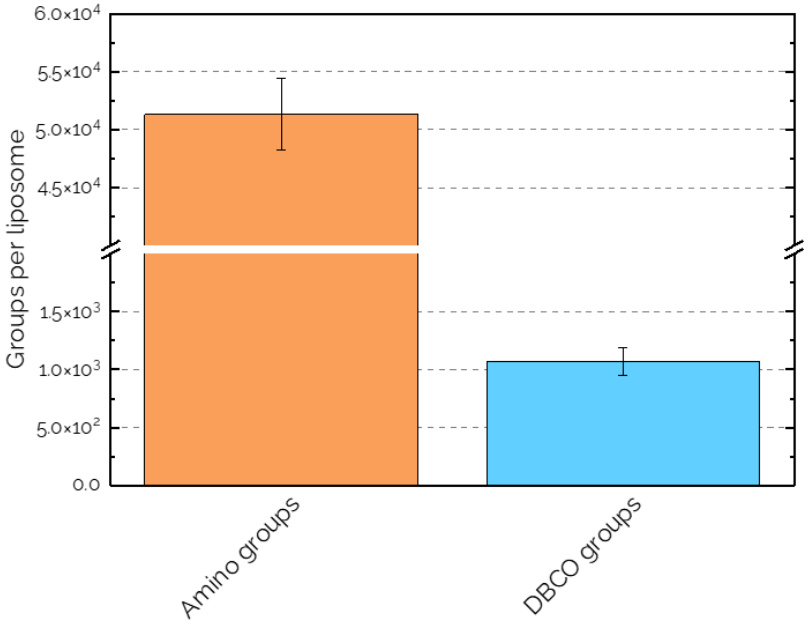

Figure 20. Quantification results of NH_2 and DBCO groups before and after liposome reaction with DBCO-PEG-NHS linker.

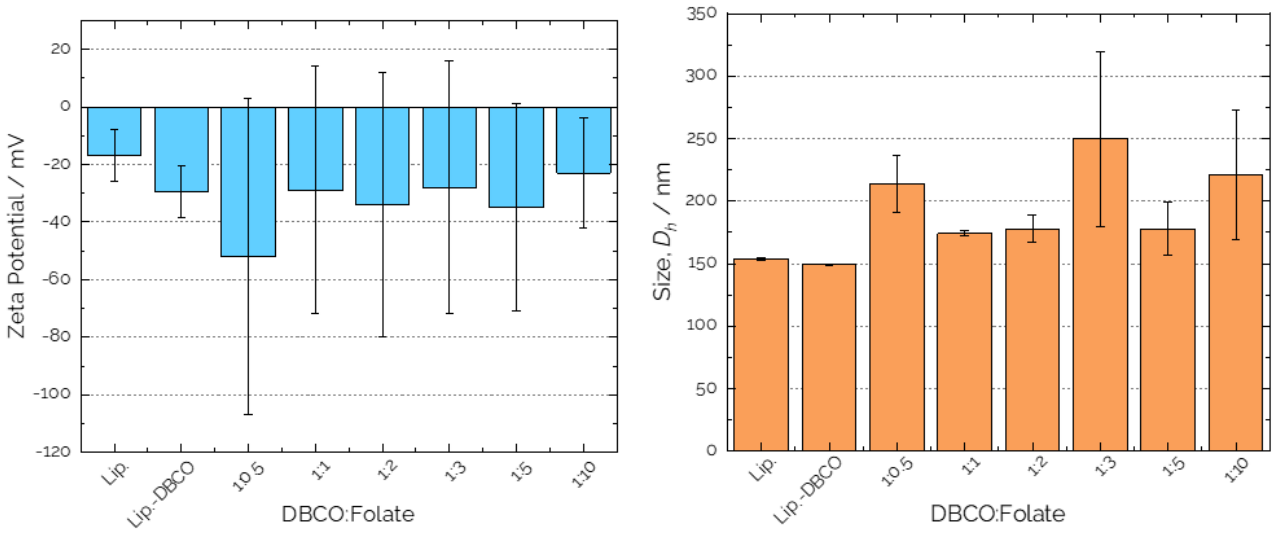

Figure 21. Physico-chemical characterization of liposomes after click chemistry folate coupling reaction. Left: Zeta potential, right: hydrodynamic diameter from dynamic light scattering.

Subsequently, again the quantification of folate groups was performed (Figure 22). As before, a decreasing trend was observed with higher DBCO:folate ratios, however not as prominent as before. This indicates that also for click chemistry, an excess of folate linker did not lead to higher conjugation yields.

This project has received funding from the European Union's Horizon 2020 research and innovation programme under grant agreement No 952183

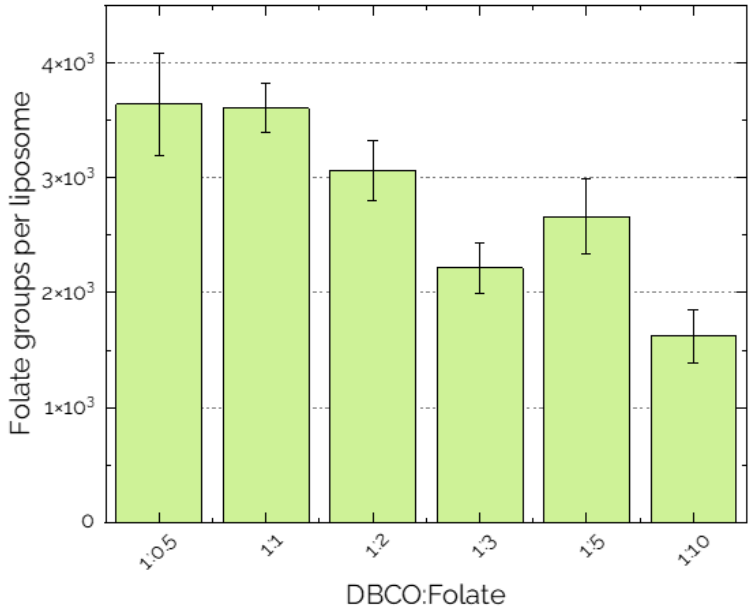

Figure 22. Quantification of folate groups results after click chemistry reaction with liposomes in different stoichiometries.

Finally, the binding of folate groups to liposomes was again investigated by flow cytometry (Figure 23). In this case, in contrast to the ApoA1 detection, a primary and a secondary antibody were used. The primary antibody was directed against folic acid (mouse, monoclonal) and the secondary antibody directed against mouse Fc fragments with fluorescent labeling (AF488). In Figure 24, the flow cytometry results of the respective samples are shown. Additionally, in Appendix II the relevant scatter plots of the functionalized liposomes with a ratio of DBCO:folate 1:1 are shown as a representative example.

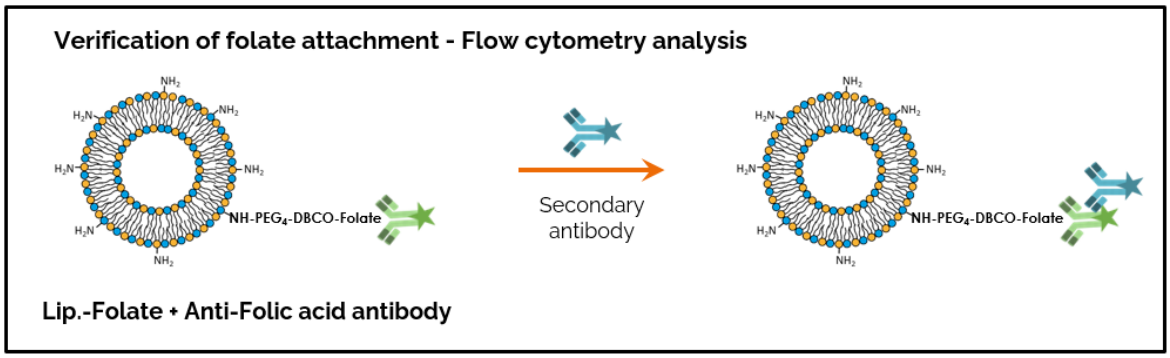

Figure 23. Schematic representation of verification of folate attachment via flow cytometry.

This project has received funding from the European Union's Horizon 2020 research and innovation programme under grant agreement No 952183

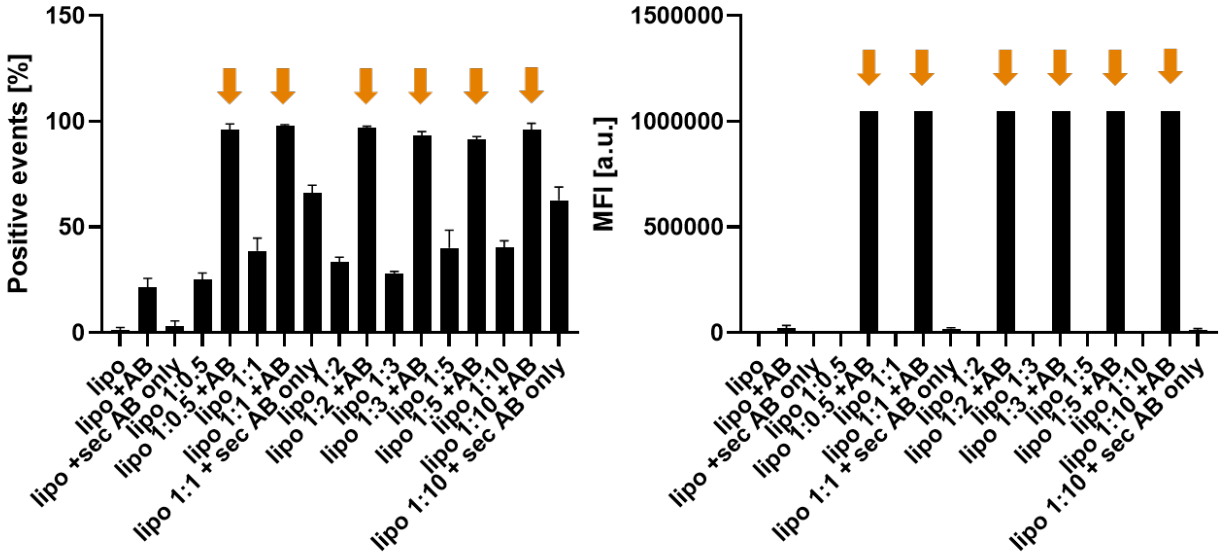

Figure 24. Verification of folate attachment to liposome surfaces by flow cytometry, of different DBCO:folate ratios from 1:0.5 to 1:10. Samples were incubated with anti-folic acid antibodies and AF488-labeled secondary antibodies and the corresponding results show the fraction of fluorescence positive events (left) and mean fluorescence intensity (MFI) of each sample (right) incubated with primary and secondary antibody (+AB, marked by orange arrows). Controls without antibodies or only with secondary antibody (+sec AB only) are included.

The flow cytometry results nicely illustrate that folate could successfully be detected on the liposome surfaces (almost all samples close to 100% fluorescence positive) and the signal intensity was very high. Additionally, also some unspecific binding of the secondary antibody was observed, which together with the high overall signals and the fact that no difference between different folate amounts was found suggests that the secondary antibody concentration needs to be lowered for further experiments. Moreover, it could be also possible that the folate attachment is already saturated at the lowest reaction ratio, which needs to be investigated in further experiments. However, the verification of folate functionalization was successful for the model liposomes.

4.2.2 NANOALGOSOMES

As described in section before, the folate conjugation strategy was developed employing model liposomes for the strategy validation. Next, we transferred the strategy to nanoalgosomes, which were already successfully used for ApoA1 functionalization before (VES4US project D4.3 “Functionalization of microalgal EVs”). In general, the functionalization procedure is, thus, analogous to the one for liposomes (see Figure 25).

This project has received funding from the European Union's Horizon 2020 research and innovation programme under grant agreement No 952183

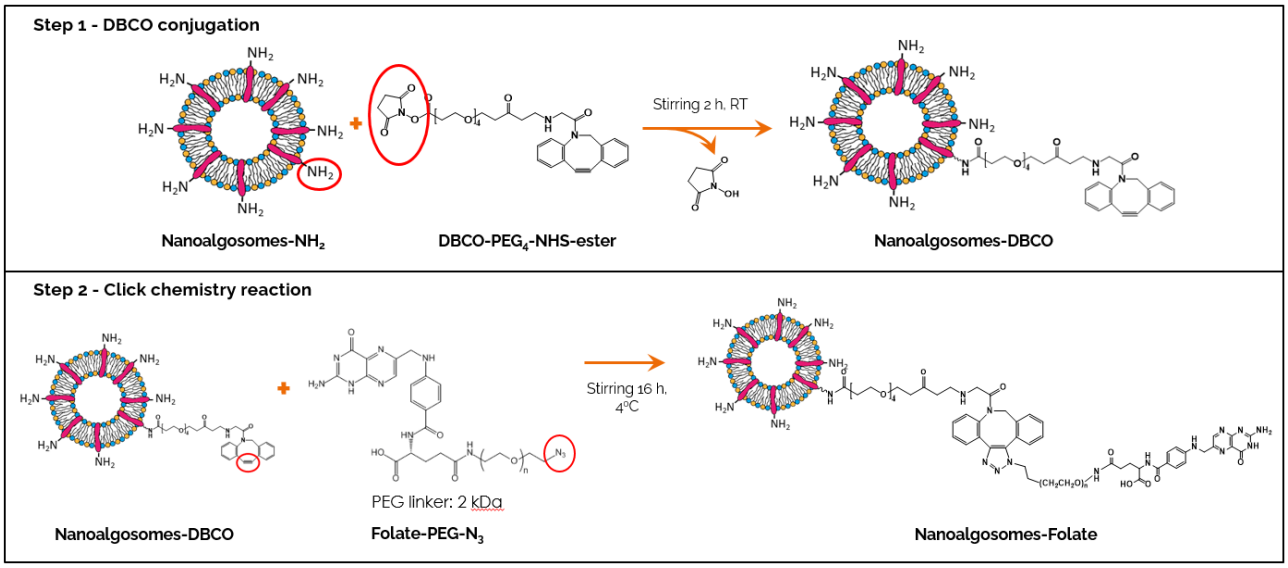

Figure 25. Functionalization reaction for folate coupling of nanoalgosomes via click chemistry.

As described above, first the quantification of amino groups was performed. Since in the case of nanoalgosomes the amino group content is less than in the other EV types, the DBCO groups to be attached need to be higher for an efficient yield. In this case, the DBCO groups were conjugated to the EV surface with a ratio of NH_2:DBCO 1:5, and subsequently quantified. The corresponding quantification results are shown in Figure 26.

Next, the reaction with the folate-PEG-azide linker was performed, using a DBCO:folate ratio of 1:2. The sample was stirred at 500-700 rpm for 48 h at 4 °C. Afterwards, the reaction mixture was purified using Amicon filters with a MWCO of 100 kDa and 3x centrifugation at 5000 g and 20 °C for 30 min. Then, the samples were again characterized regarding size and surface charge (see Table 6). In this case, no aggregation was observed, which hints at a good sample quality.

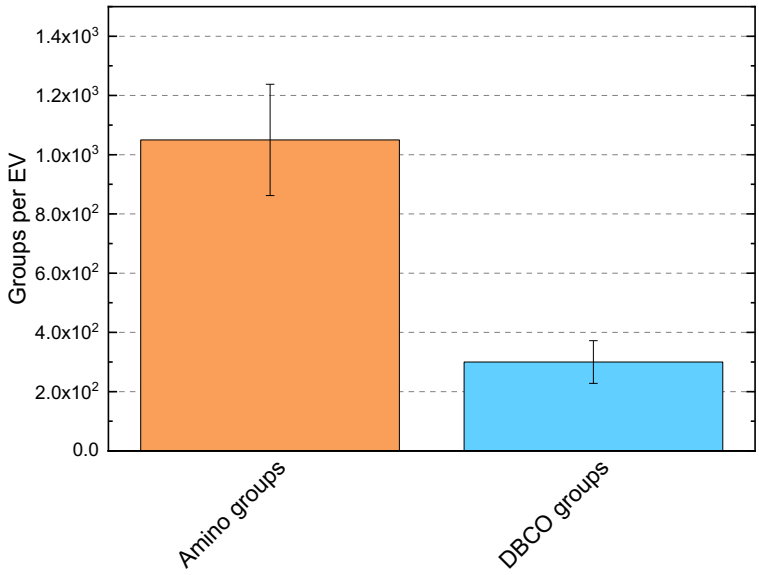

This project has received funding from the European Union's Horizon 2020 research and innovation programme under grant agreement No 952183

Figure 26. Quantification results of NH_2 and DBCO groups before and after nanoalgosome reaction with DBCO-PEG-NHS linker.

Table 6. Physico-chemical characterization of nanoalgosomes before and after the different functionalization steps.

Sample	Size: d (nm)	PdI	Zeta Potential (mV)
Nanoalgosomes	50 - 150	0.21	-24 ± 20
Nanoalgosomes-DBCO:NH_2 5:1	40 - 150	0.22	-19 ± 41
Nanoalgosomes-Folate:DBCO 2:1	40 – 150	0.24	-22 ± 18

Subsequently, folate groups were quantified via absorbance in the functionalized sample as well as the unfunctionalized nanoalgosomes as negative control. The obtained numbers are shown in Figure 27, where a clear increase of folate in the functionalized nanoalgosome sample was present.

Finally, also for nanoalgosomes the verification of folate binding was conducted via flow cytometry. Figure 28 shows the results obtained from the measurements.

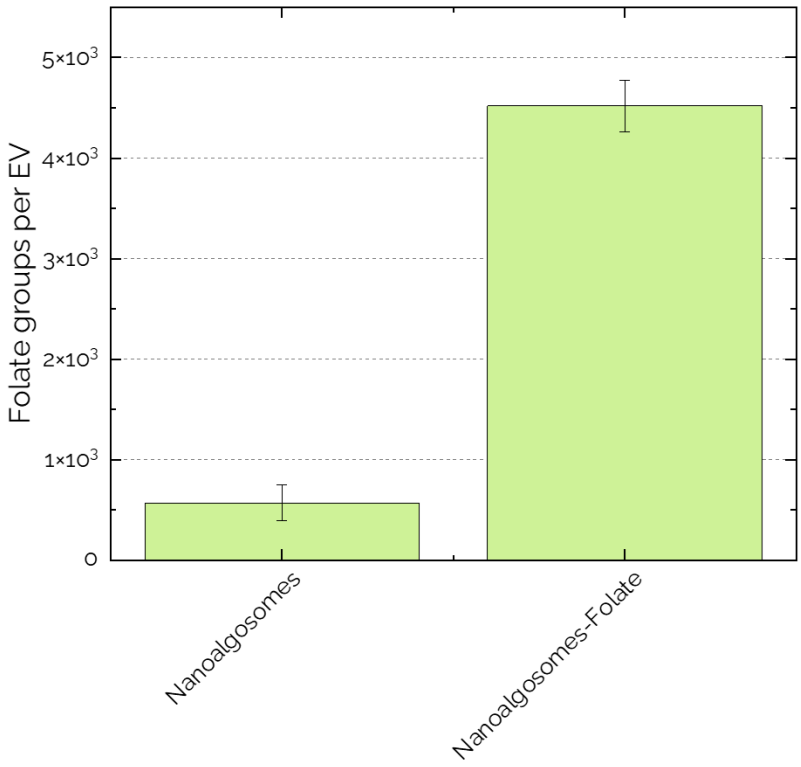

Figure 27. Quantification of folate groups results after click chemistry reaction with nanoalgosomes together with negative control.

This project has received funding from the European Union's Horizon 2020 research and innovation programme under grant agreement No 952183

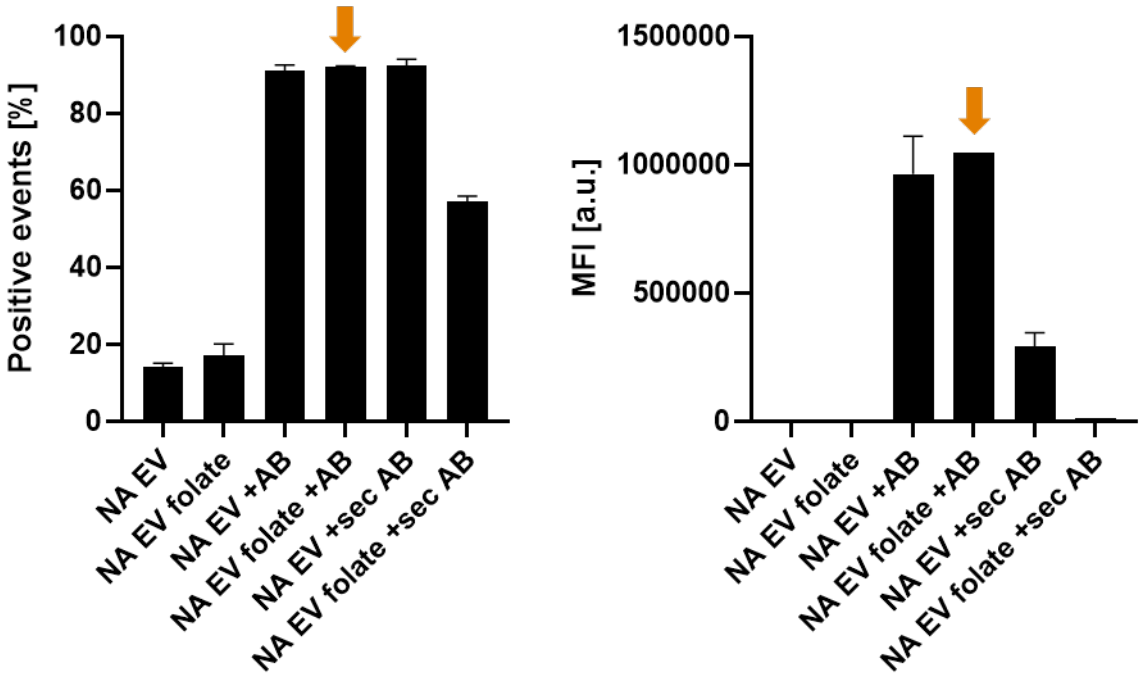

Figure 28. Verification of folate attachment to nanoalgosome surfaces by flow cytometry. Samples were incubated with anti-folic acid antibodies and AF488-labeled secondary antibodies and the corresponding results show the fraction of fluorescence positive events (left) and mean fluorescence intensity (MFI) of each sample (right) incubated with primary and secondary antibody (+AB), marked by orange arrows). Additionally, controls without antibodies or only with secondary antibody (+sec AB) are included.

As reported above for the liposomes, also in this case high fluorescence signals were observed for the samples functionalized with folate, which hints at successful coupling. However, also in some controls, high signals are observed, which, again, probably suggests that antibody concentration still needs to be optimized in order to decrease unspecific adsorption and obtain final proof of successful conjugation. Moreover, folate has been proven to be naturally enriched in some microalgae[6], which could lead to AB binding in control samples. This has to be further investigated in the future. Overall, we are optimistic that also in the case of nanoalgosomes the coupling with folate was successful.

5. CONCLUSIONS

In this deliverable, we have reported two different strategies for exogenous functionalization EV membranes, depending on what type of molecule needs to be conjugated. For the first strategy, we have successfully expanded the existing protein (ApoA1) functionalization in two ways: 1) transfer to other EV sources (MSC-EVs and RBC-EVs) and 2) scale-up of the functionalization procedure (RBC-EVs).

This project has received funding from the European Union's Horizon 2020 research and innovation programme under grant agreement No 952183

For folate functionalization, a change of strategy was necessary, but finally we were able to show that folate can successfully be detected on EV membranes. Therefore, the objective of the task has been fairly achieved.

One major difficulty for all the proposed functionalization strategies are the involved washing and purification steps because they always result in significant loss of material and broadening of the EV size distribution, meaning lowering the final yield and of the quality of the products.

Therefore, in parallel to provide functionalized samples for next use in the project, we will work in the next towards protocol optimization.

We will also explore the out-of-the-box option of the direct functionalization of the magnetic nanoparticle-EV hybrids (evMBDs), which was not foreseen in the original GA. This should result in less preparation steps. For example, facilitating the purification significantly, as the products could easily be separated in one passage from the reaction solution by a magnet. Overall, this approach should result in much more defined products (regarding size distribution, but also e.g. functionalization density with higher yield.

This project has received funding from the European Union's Horizon 2020 research and innovation programme under grant agreement No 952183

6. REFERENCES

1. J. A. Welsh, E. Van Der Pol, G. J. A. Arkesteijn, M. Bremer, A. Brisson, F. Coumans, F. Dignat-George, E. Duggan, I. Ghiran, B. Giebel, A. Görgens, A. Hendrix, R. Lacroix, J. Lannigan, S. F. W. M. Libregts, E. Lozano-Andrés, A. Morales-Kastresana, S. Robert, L. De Rond, T. Tertel, J. Tigges, O. De Wever, X. Yan, R. Nieuwland, M. H. M. Wauben, J. P. Nolan and J. C. Jones, *Journal of Extracellular Vesicles*, 2020, **9**, 1713526.
2. J. A. Welsh, G. J. A. Arkesteijn, M. Bremer, M. Cimorelli, F. Dignat-George, B. Giebel, A. Görgens, A. Hendrix, M. Kuiper, R. Lacroix, J. Lannigan, T. G. van Leeuwen, E. Lozano-Andrés, S. Rao, S. Robert, L. de Rond, V. A. Tang, T. Tertel, X. Yan, M. H. M. Wauben, J. P. Nolan, J. C. Jones, R. Nieuwland and E. van der Pol, *Journal of Extracellular Vesicles*, 2023, **12**, e12299.
3. M. C. Lo Giudice, L. M. Herda, E. Polo and K. A. Dawson, *Nature Communications*, 2016, **7**, 13475.
4. M. Gai, J. Simon, I. Lieberwirth, V. Mailänder, S. Morsbach and K. Landfester, *Polymer Chemistry*, 2020, **11**, 527-540.
5. O. Modupe, J. B. Maurras and L. L. Diosady, *Journal of Agriculture and Food Research*, 2020, **2**, 100060.
6. D. V. Woortman, T. Fuchs, L. Striegel, M. Fuchs, N. Weber, T. B. Brück and M. Rychlik, *Frontiers in Bioengineering and Biotechnology*, 2020, **7**.

This project has received funding from the European Union's Horizon 2020 research and innovation programme under grant agreement No 952183

APPENDIX I

CHARACTERIZATION DATA OF EV BATCHES

A

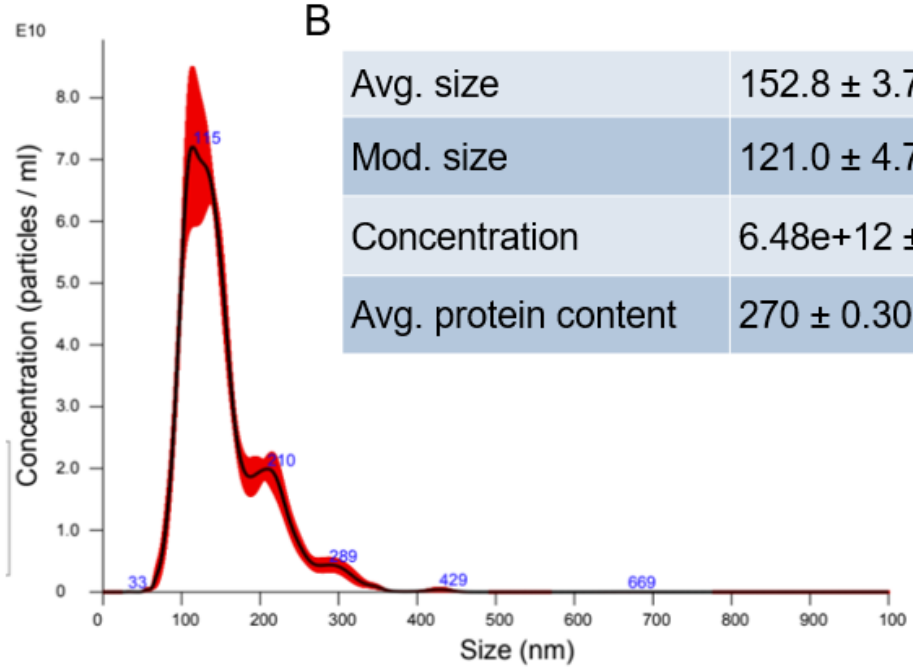

B

Avg. size	152.8 ± 3.7 nm
Mod. size	121.0 ± 4.7 nm
Concentration	6.48e+12 ± 3.63e+11 p/mL
Avg. protein content	270 ± 0.30 ug/mL

C

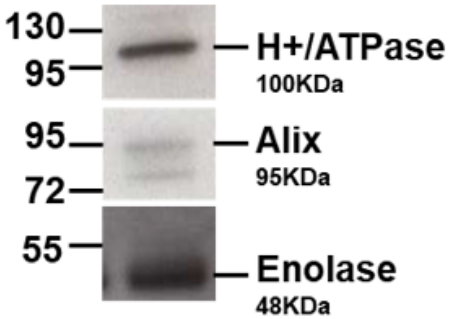

D

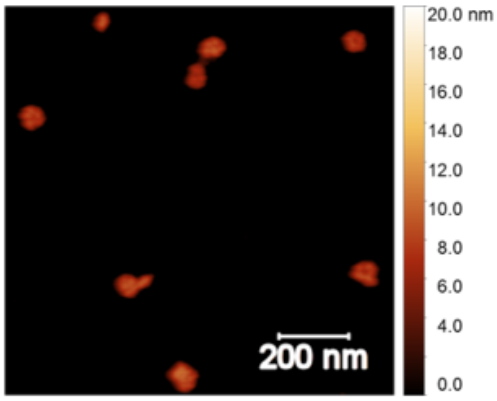

Figure I.1. Characterization of the sample "SG3" (nanoalgosomes). **A)** NTA of the sample. **B)** Size, concentration, and average protein content of the preparation. **C)** Representative molecular markers. D) Representative AFM micrograph.

This project has received funding from the European Union's Horizon 2020 research and innovation programme under grant agreement No 952183

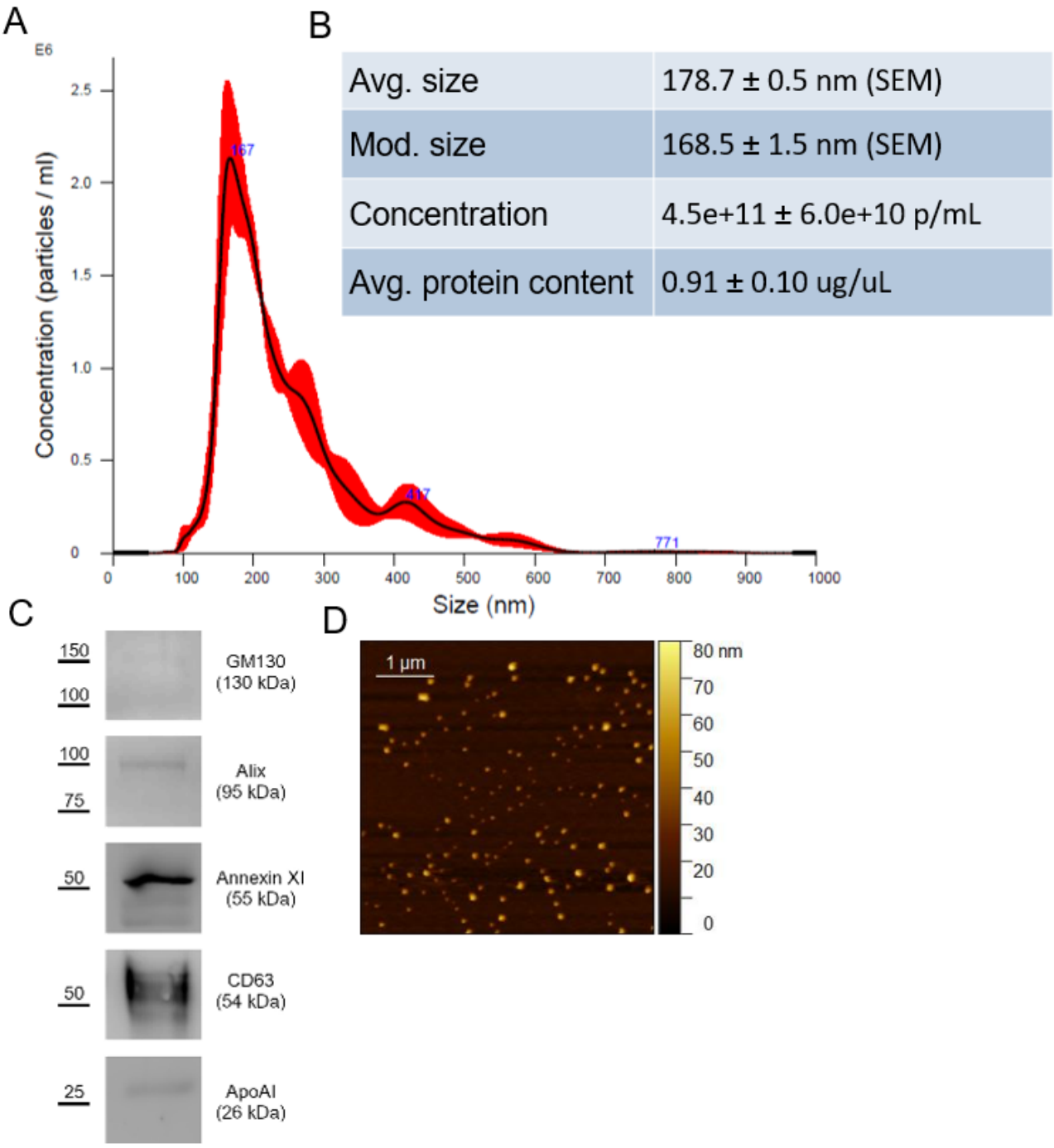

Figure I.2. Characterization of the sample "EV-3D16_1" (MSC EVs). **A)** NTA of the sample. **B)** Size, concentration, and average protein content of the preparation. **C)** Representative molecular markers. **D)** Representative AFM micrograph.

This project has received funding from the European Union's Horizon 2020 research and innovation programme under grant agreement No 952183

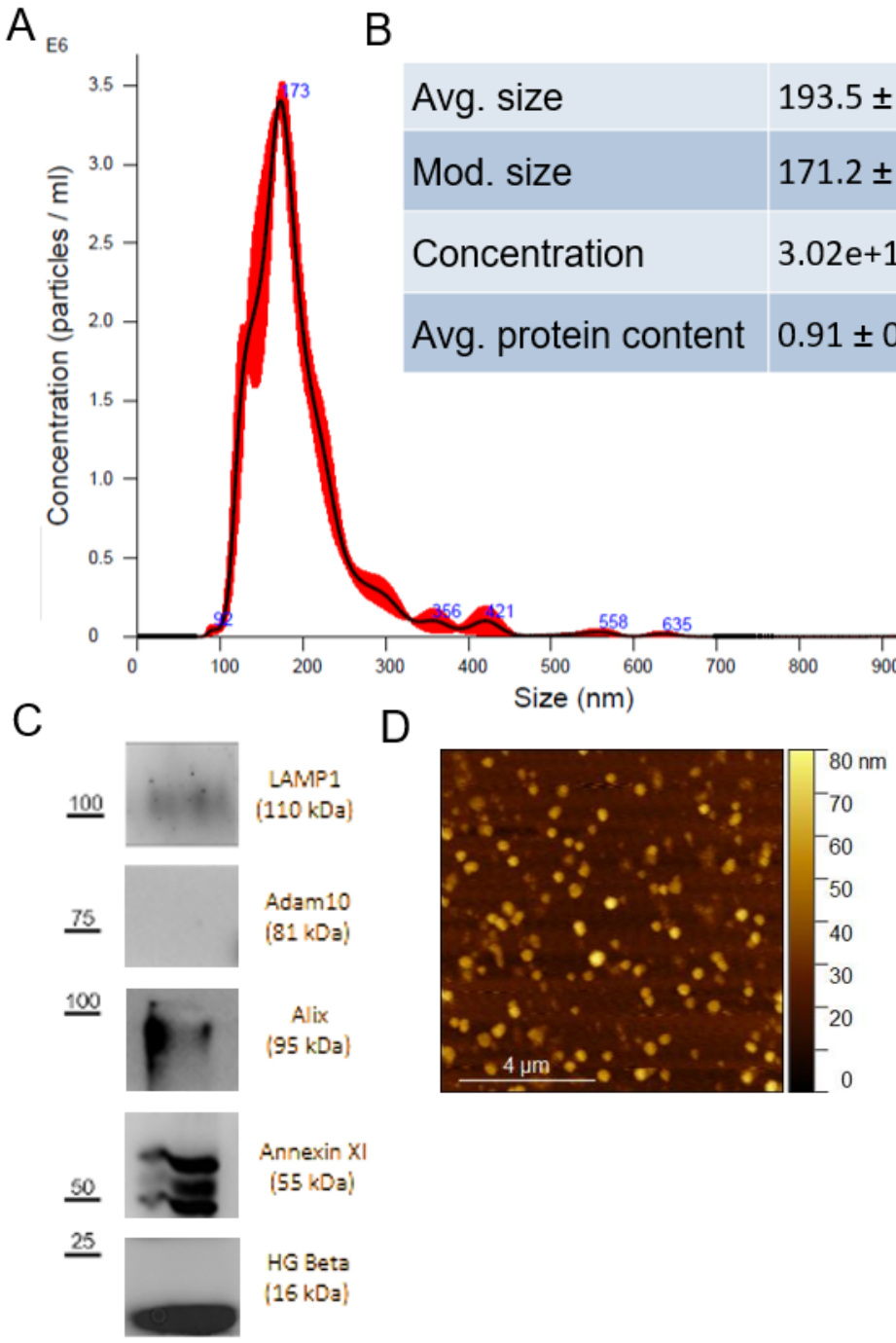

Figure I.3. Characterization of the sample "AM_RBC_001_12" (RBC-EVs). **A)** NTA of the sample. **B)** Size, concentration, and average protein content of the preparation. **C)** Representative molecular markers. **D)** Representative AFM micrograph.

This project has received funding from the European Union's Horizon 2020 research and innovation programme under grant agreement No 952183

APPENDIX II

FLOW CYTOMETRY GATING STRATEGIES

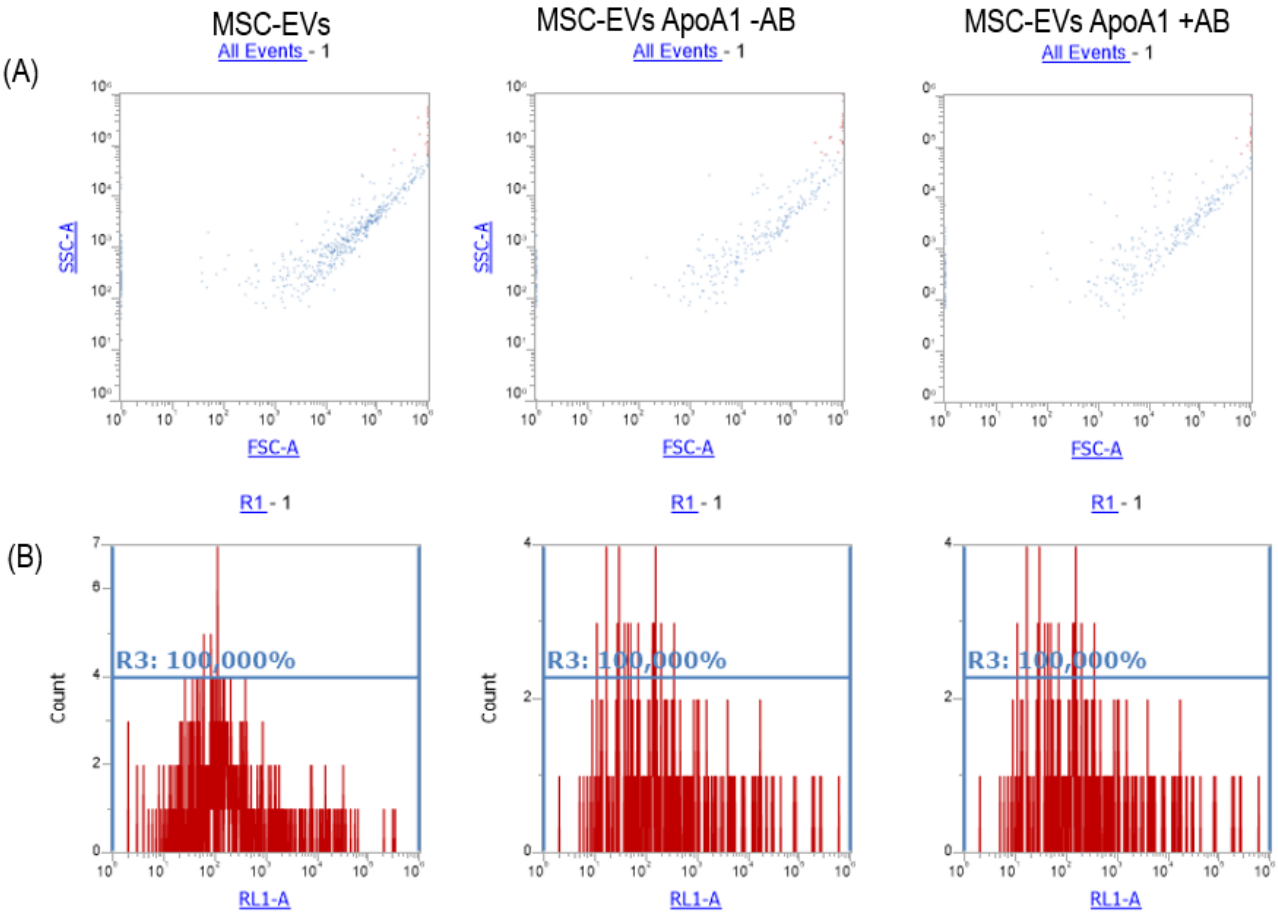

Figure II.1. (A) Particle population was identified based on the area of forward (FSC) and sideward (SSC) scatter for MSC-Evs (sample "EV-3D16_1"), MSC-EVs functionalised with ApoA1 and anti-ApoA1 stained MSC EVs functionalized with ApoA1. **(B)** A histogram was plotted for the area of RL1-detected fluorescence. The median fluorescence intensity was determined across all events and used to quantify antibody binding.

This project has received funding from the European Union's Horizon 2020 research and innovation programme under grant agreement No 952183

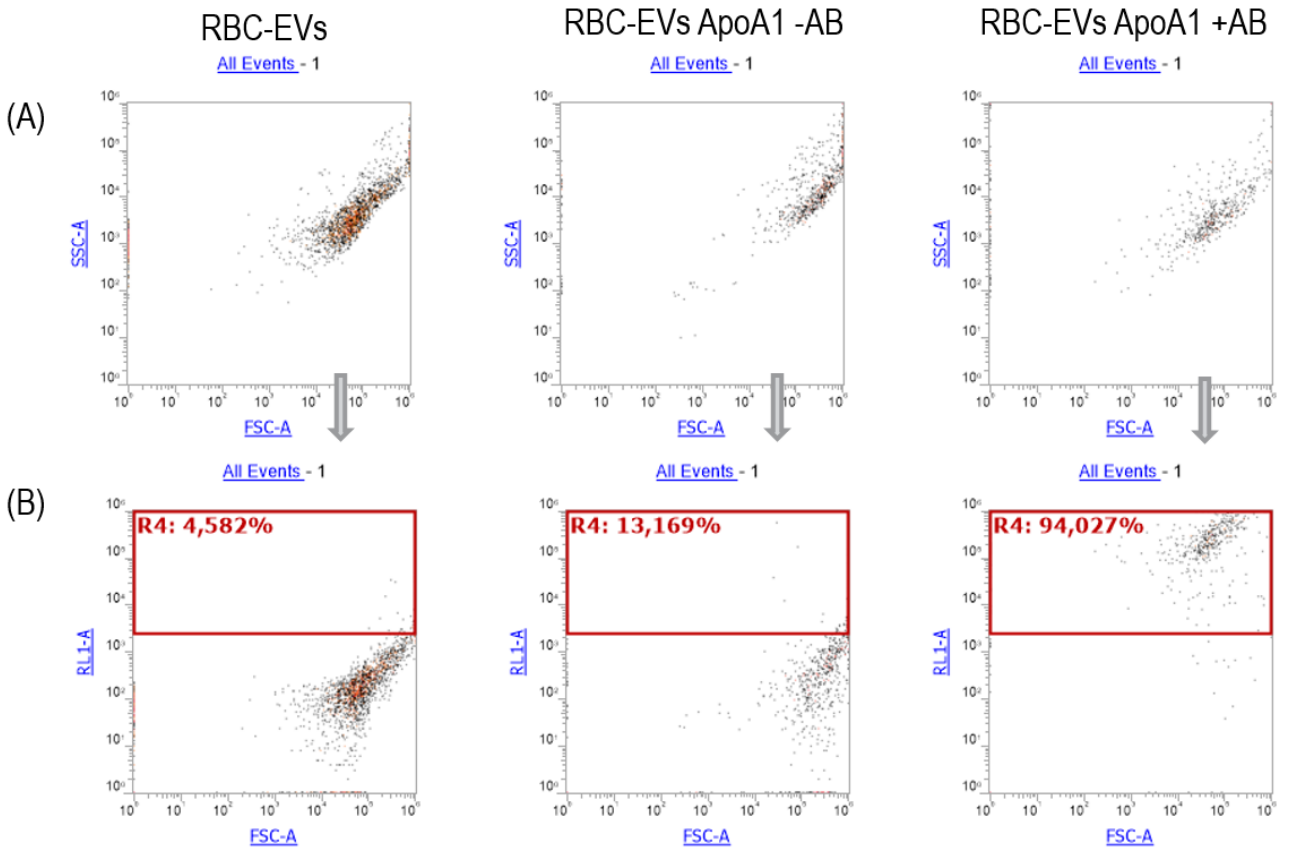

Figure II.2. (A) Particle population was identified based on the area of forward (FSC) and sideward (SSC) scatter for RBC-Evs (AM_RBC_001_12), RBC-EVs functionalized with ApoA1 and anti-ApoA1 stained RBC-EVs functionalised with ApoA1. **(B)** The fluorescent gate was set based on plotting the area of FSC against the area of the fluorescent channel RL1. As negative control, non-functionalized, non-antibody-stained RBC EVs were gated to have 4 % of positive events. The percentage of positive events was used to quantify antibody binding.

This project has received funding from the European Union's Horizon 2020 research and innovation programme under grant agreement No 952183

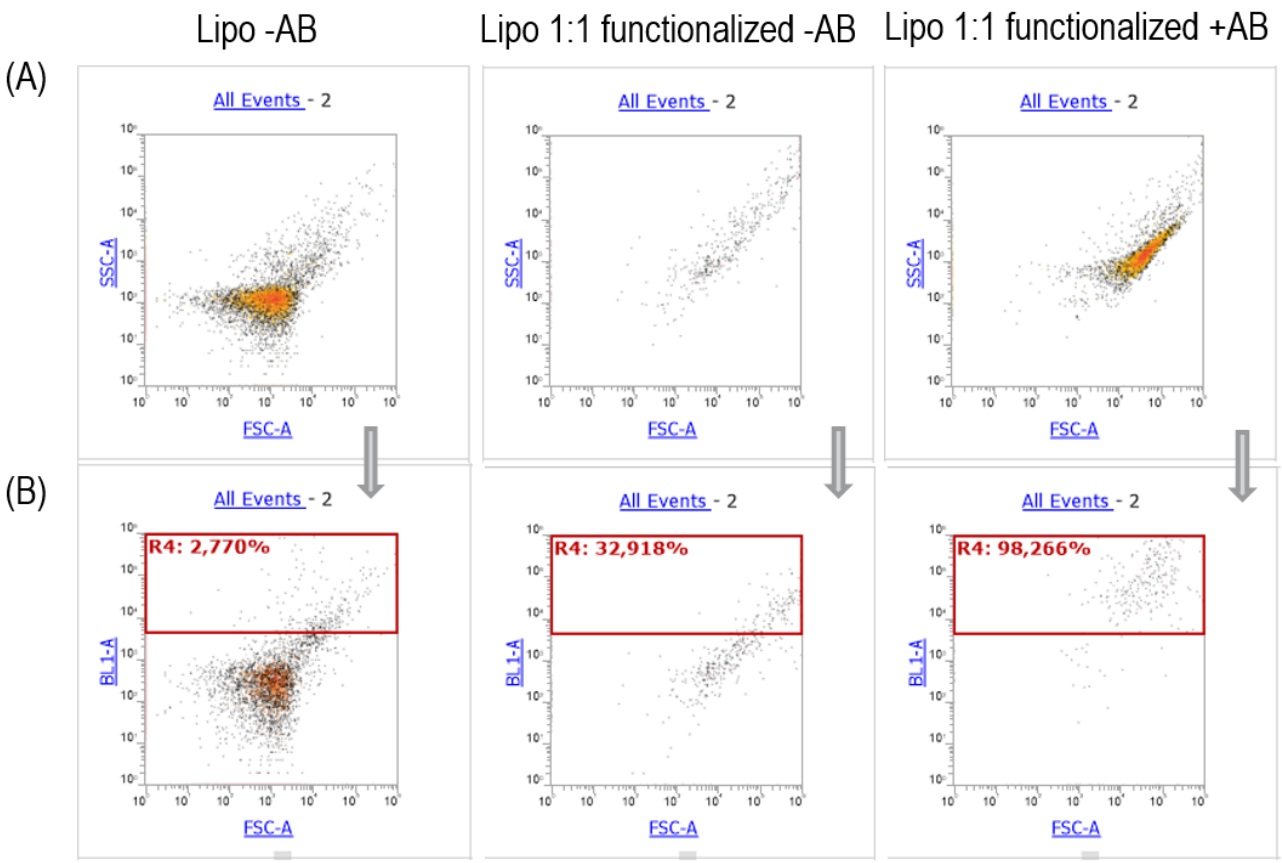

Figure II.3. (A) Particle population was identified based on the area of forward (FSC) and sideward (SSC) scatter for liposomes, liposomes functionalized with folate (DBCO:folate 1:1) and anti-folate stained liposomes functionalized with folate. **(B)** The fluorescent gate was set based on plotting the area of FSC against the area of the fluorescent channel RL1. As negative control, non-functionalized, non-antibody-stained RBC EVs were gated to have 2 % of positive events. The percentage of positive events was used to quantify antibody binding.

This project has received funding from the European Union's Horizon 2020 research and innovation programme under grant agreement No 952183